

FINAL TECHNICAL REPORT

CHARGED PARTICLE RADIATION DAMAGE IN SEMICONDUCTORS, XII:

EFFECTS OF HIGH ENERGY ELECTRONS IN

SILICON AND SILICON SOLAR CELLS

25 MAY 1966

4161-6023-R0000

Contract No. NAS5-3805

NATIONAL AERONAUTICS AND SPACE ADMINISTRATION

GODDARD SPACE FLIGHT CENTER

TRW SYSTEMS

FINAL TECHNICAL REPORT

CHARGED PARTICLE RADIATION DAMAGE IN SEMICONDUCTORS, XII: EFFECTS OF
HIGH ENERGY ELECTRONS IN SILICON AND SILICON SOLAR CELLS

by

J. R. Carter
R. G. Downing
H. Flicker

25 May 1966

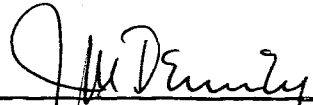
4161-6023-R0000

Contract No. NAS5-3805

National Aeronautics and Space Administration
Goddard Space Flight Center

Radiation Effects Department
Solid State Physics Laboratory

Approved:



Joseph M. Denney, Director
Solid State Physics Laboratory

TRW SPACE TECHNOLOGY LABORATORIES

One Space Park
Redondo Beach, California

ACKNOWLEDGEMENTS

This report covers work performed under Contract NAS5-3805 during the period from 26 May 1965 to 26 May 1966. We would like to acknowledge the helpful guidance of, and discussions with, Mr. Milton Schach, Dr. Pao Fang, and their associates of NASA-Goddard Space Flight Center during the conduct of this program. We would also like to acknowledge the cooperation and assistance of the many semiconductor organizations who provided the material and devices upon which these studies were based.

ABSTRACT

29751

A broad experimental program has been conducted to study the effects of electron bombardment in silicon and silicon solar cells. Using Hall effects measurements, it has been found that the defect introduction rate of the $E_v + 0.3\text{ev}$ level is independent of dopant material in crucible grown p-type silicon. Since this level is not found in float zone p-type silicon, it appears that the defect does not involve a dopant impurity and depends on the presence of oxygen for its formation. These findings are consistent with previous suggestions that the silicon K center and the $E_v + 0.3\text{ev}$ level are related to the same defect and also with the currently proposed model that the K center is a double oxygen, double vacancy complex, or a double A center. Annealing experiments indicate that the 0.3 ev level begins to anneal rapidly around 500°C with complete annealing at 500°C to 600°C in low dislocation material. In high dislocation material the annealing occurs in two stages at 350° to 400°C and 550° to 600°C . Complete annealing of n/p solar cells is also observed to occur in the 400°C range. Since reasonably high dislocation densities are produced in the production of solar cells, the similar annealing characteristics observed lend further support to the relationship between the 0.3 ev level and the degradation of n/p solar cells. In addition, a series of experiments were performed on the dependence of solar cell degradation under electron bombardment on irradiation temperature. It is observed that both p/n and n/p solar cells exhibit

over

ERRATA SHEET

FINAL TECHNICAL REPORT

CHARGED PARTICLE RADIATION DAMAGE IN SEMICONDUCTORS, XII: EFFECTS OF
HIGH ENERGY ELECTRONS IN SILICON AND SILICON SOLAR CELLS

The following corrections should be made in this report:

(1) Page 14 - Second complete paragraph

$E_V - 0.17\text{ev}$ in the first sentence should be changed to
 $E_C - 0.17\text{ev}$.

(2) Page 26 - First complete paragraph

$E_V - 0.3\text{ev}$ in the last sentence should be changed to
 $E_V + 0.3\text{ev}$.

(3) Page 27 - First paragraph

$E_C + 0.3\text{ev}$ in the first sentence should be changed to
 $E_V + 0.3\text{ev}$.

recombination center introduction rates which are independent of temperature over a range of 77°K to 373°K for p/n solar cells and over a range of 198°K to 373°K for n/p solar cells. At 77°K n/p solar cells exhibit an apparent factor of 5 increase in degradation rate. The recombination center responsible for this effect can be produced and observed only at 77°K and is not stable at higher temperatures.

TABLE OF CONTENTS

	<u>Page</u>
I. INTRODUCTION	1
II. EFFECT OF IMPURITIES ON PRODUCTION OF THE $E_v + 0.3$ ev LEVEL. . . .	2
III. ANNEALING OF ELECTRON INDUCED ENERGY LEVELS IN SILICON	8
IV. THERMAL ANNEALING OF ELECTRON IRRADIATED SOLAR CELLS	11
V. ELECTRON IRRADIATION OF FLOAT ZONE n-TYPE SILICON.	15
VI. TEMPERATURE DEPENDENCE OF ELECTRON DAMAGE IN SOLAR CELLS	18
VII. RECOMBINATION CENTERS IN ELECTRON IRRADIATED SOLAR CELLS	22
TABLE 1.	28
REFERENCES	59

LIST OF ILLUSTRATIONS

<u>Figure</u>		<u>Page</u>
1	Hall Coefficient of Electron Irradiated Boron Doped Crucible Grown p-type Silicon	
2	Hall Coefficient of Electron Irradiated Aluminum Doped Crucible Grown p-type Silicon	
3	Hall Coefficient of Electron Irradiated Gallium Doped Crucible Grown p-type Silicon	
4.	Hall Coefficient of Electron Irradiated Indium Doped Crucible Grown p-type Silicon	
5	Hall Coefficient of Electron Irradiated Gadolinium Doped Crucible Grown p-type Silicon	
6	Hall Coefficient of Electron Irradiated Boron Doped Float Zone p-type Silicon	
7	Hall Coefficient Data for Isochronal Annealing of Electron Irradiated Crucible Grown n-type Silicon	
8	Isochronal Annealing of Electron Irradiated Crucible Grown n-type Silicon	
9	Isochronal Annealing of Electron Irradiated Crucible Grown p-type Silicon (130 Ω -cm, low dislocation)	
10	Isochronal Annealing of Electron Irradiated Crucible Grown p-type Silicon (15 Ω -cm, low dislocation)	
11	Hall Coefficient Data for Isochronal Annealing of Electron Irradiated, Crucible Grown p-type Silicon (15 Ω -cm, high dislocation)	
12	Isochronal Annealing of Electron Irradiated Electron, Crucible Grown p-type Silicon (15 Ω -cm, high dislocation). . .	
13	Isochronal Annealing of Hoffman n/p Solar Cells	
14	Isochronal Annealing of R.C.A. n/p Solar Cells.	
15	Heat Treatment of an Unirradiated R.C.A. n/p Solar Cell . . .	
16	Isochronal Annealing of Texas Instruments n/p Solar Cells . .	

17	Isothermal Annealing of Hoffman n/p Solar Cells
18	Isothermal Annealing of Hoffman n/p Solar Cells (Semi-logarithmic Plot)
19	Arrhenius Plot for Hoffman n/p Solar Cells
20	Electron Damage Defect Introduction Rate for n-type Float Zone Silicon
21	Carrier Concentration Versus Reciprocal Temperature for Electron Irradiated n-type Float Zone Silicon Sample
22	Donor Ionization Energy for an Electron Irradiated Float Zone n-type Silicon Sample.
23	Experimental Apparatus for Electron Irradiation of Solar Cell at Various Temperature
24	Close Up View of Solar Cell Irradiation Apparatus
25	Damage Rate of Solar Cells for 1 MeV Electrons at Various Temperatures.
26	Room Temperature Short Circuit Currents for Solar Cell Irradiated at Various Temperatures
27	Dependence of Lifetime on Reciprocal Temperature, Unirradiated p/n Silicon Solar Cell.
28	Dependence of Lifetime on Reciprocal Temperature, Electron Irradiated p/n Silicon Solar Cell
29	Dependence of Lifetime on Reciprocal Temperature Unirradiated n/p Silicon Solar Cell.
30	Dependence of Lifetime on Reciprocal Temperature Electron Irradiated n/p Silicon Solar Cell

I. INTRODUCTION

The objective of the efforts presented in this report was to gain further understanding of defects in electron irradiated silicon. Many investigations of recombination in electron irradiated silicon have been reported.¹⁻⁵ Because of the complexity involved in the nature of recombination statistics, conflicting results have often been observed. However, by using direct and indirect methods, several conclusions can be reached regarding the defects involved in recombination. Considerable information has been gathered by these means. The problem now is to rationalize the data obtained by these various methods in order to resolve those areas where conflicting evidence exists.

The studies completed in this program cover several aspects of radiation defects. Although most of this work is of a more basic nature, some of the results can be useful in engineering problems or applications. The first four sections cover studies which were designed to give information about characteristics and structure of major radiation defects. This work employs mainly the effects of variation of dopants in the silicon and the study of the kinetics of thermal annealing of defects. The remaining sections cover studies relating to the recombination process in electron irradiated silicon.

II. EFFECT OF IMPURITIES ON PRODUCTION OF THE $E_v + 0.3\text{ev}$ LEVEL

The radiation defects present in silicon at room temperature have been shown to be considerably more complicated than simple vacant lattice sites and interstitial silicon atoms which are stable only at the very lowest temperatures, if at all. The first stable defect to be well characterized was the Si-A or Si-B1 center.⁶ This defect was proven to be an oxygen-vacancy pair. The defect is also an electrically active acceptor which can remove electrons from the conduction band with an activation energy of 0.17 ev. The complex nature of this defect is typical of the defects found at room temperature. A few such defects have been characterized as to crystalline and electronic structure. The status of this subject was reviewed by Watkins at the Paris conference.⁷ This laboratory has devoted considerable effort to study of a donor level 0.3 ev above the valence for conduction band.^{1,2,8,9} This defect is the principle carrier removal site during electron irradiation of crucible grown p-type silicon. The defect responsible for this energy level is also believed to be related to the Si-K center resonance.¹⁰ This defect is of particular interest because its introduction rate and the degradation rate of minority carrier lifetime in n/p solar cells have the identical steep electron energy dependence. Since the nature of the recombination center in irradiated p-type silicon is still in doubt, the energy dependence data indicates that the 0.3 ev level may be involved in recombination.

Because of its possible role in recombination, it is desirable to know more about the structure of the $E_v + 0.3\text{ ev}$ level. Since the level can only be observed in p-type silicon, it is possible to vary the

acceptor atom used in doping the crystal. If dopant atoms are included in the radiation defect complex, one might expect to see some variation in the defect introduction rate when various chemical dopants are used. Likewise, if oxygen is involved in the defect complex, changes in the oxygen concentration should affect the introduction rate of the defect. Studies of this type not only clarify defect structures, but indicate possible ways to control or minimize the radiation damage. In addition, the results may offer confirmation of the relation between the K center and the 0.3 ev level.

Several p-type silicon crystals were grown by the crucible method by Monosilicon, Division of Wacker Chemical. The dopants used were boron, aluminum, gallium, indium, and gadolinium. An attempt was made to grow all the crystals with a resistivity of 10 ohm-cm; however, some variation was encountered. All crystals had dislocation concentrations below $100/\text{cm}^2$, except for the boron doped crystal which had $10^4/\text{cm}^2$ by etch pit count. The crystals were fabricated into bridge samples for Hall effect measurements. The instrumentation details of the Hall measurement have been discussed in previous reports.⁵ The irradiations were done on the TRW 1 Mev Van de Graaff at an energy of 1 MeV at room temperature. Beam currents were measured with a Faraday cup and integrating amplifier arrangement. The Hall coefficient was measured as a function of temperature before irradiation. The samples were then irradiated with care to avoid the effects of any beam heating. After irradiation, the Hall measurements are repeated. The analysis of this type of data has been covered by Wertheim² and Hill⁸.

The experimental results of irradiation of the crucible grown silicon is shown in Figures 1 through 5. The data for the boron doped, high dislocation silicon is shown in Figure 1. The vertical axis represents the ratio of before and after irradiation Hall coefficients. This parameter eliminates the temperature dependent Hall factor from the analysis. The resulting curve can be interpreted as if it were carrier concentration as a function of reciprocal temperature. The data is consistent with a single donor level at $E_v + 0.3\text{ev}$. An introduction rate of 0.025 cm^{-1} was measured for the defect.

The data for the aluminum doped sample is shown in Figure 2. In this figure, reciprocal Hall coefficient is plotted on the vertical axis. The data again indicates a donor level at $E_v + 0.3\text{ev}$ with an introduction rate of 0.028 cm^{-1} . In Figure 3, similar data is shown for a gallium doped sample. After irradiation, this data also shows evidence of the $E_v + 0.3\text{ev}$ level. The introduction rate for the level in this sample is 0.028 cm^{-1} .

The data for the indium doped silicon is presented in Figure 4. The curve for the unirradiated sample is different from those previously discussed. Normally the Hall coefficient changes very little in the range between 100° to 300°K for unirradiated silicon. A slight slope is usually found because of the temperature dependence of the Hall factor. The unirradiated indium doped silicon shows a large inflection, typical of a deep level at 0.16 ev above the valance band. Normal dopants such as boron or aluminum have very shallow energy levels. This means that the

Hall coefficient will not change greatly near room temperature because the Fermi level is remote from the acceptor level. In the case of indium this is not true. The indium acceptor level is 0.16 ev above the top of the valence band. Above room temperature most of the indium atoms are ionized and the reciprocal Hall coefficient is large. At about 180°K ($\frac{1000}{T} = 5.6$) the Fermi level is 0.16 ev above the valence band and half the indium atoms are ionized. At still lower temperatures, the indium atoms are neutral and the reciprocal Hall coefficient is much lower but not changing rapidly.

Because of the differences involved with indium, the interpretation of the irradiation results is complicated. It can be seen from Figure 4 that the Fermi level locks onto the indium level after irradiation. This limits the data which can be obtained from the sample. It is clear, however, that the electron irradiation has introduced a deep acceptor in the forbidden band. This has caused the Fermi level to move further from the valence band edge. The introduction rate of the irradiation produced deep acceptor level is estimated to be about 0.023 cm^{-1} . Although the $E_v + 0.3 \text{ ev}$ level cannot be detected, it is not unreasonable to assume that it is the defect responsible for the observed removal rate. The data from irradiation of the gadolinium doped silicon is shown in Figure 5. The analysis of this data again indicates a donor level at $E_v + 0.3 \text{ ev}$ with an introduction rate of 0.028 cm^{-1} .

Figure 6 contains the data for irradiation of a float zone silicon crystal. The results show evidence of two or more donor levels introduced as a result of the irradiation. One level was introduced at

approximately $E_v + 0.20\text{ev}$ with an introduction rate of 0.010 cm^{-1} .

In addition, one or more donor levels are introduced deep in the band gap.

At the highest temperature reached, the Fermi level is 0.31 ev above the top of the valence. It is apparent from the data that the deep radiation damage level must be at least a few kT deeper than 0.31 ev .

This would place the energy level further than 0.35 ev from the band gap.

The introduction rate for the deep level is 0.018 cm^{-1} .

Two conclusions can be reached from the data presented. The introduction rate of the 0.3 ev level does not vary significantly when various chemical dopants are utilized as the principal acceptor. The slight differences observed are small enough to be attributed to experimental data scatter. Since the introduction rate appears to be independent of the acceptor atom, the defect complex associated with the 0.3 ev level does not involve atoms of the dopant. If the 0.3 ev level is involved in recombination in electron damaged silicon, it is not likely that radiation damage could be reduced by substitution of one acceptor for another.

The results found in the float zone silicon are particularly interesting in as much as the $E_v + 0.3\text{ev}$ level was not detected. Evidence was found for two or more energy levels which are not found in crucible grown silicon. The presence of an $E_v + 0.20\text{ev}$ level in irradiated float zone silicon has been reported by other investigators.^{11,12} However, the structure of the defect is not known. The introduction rate is much lower than that of the 0.3 ev level. No conclusions can be reached

about the deep level detected. It is interesting to note that the introduction rate of the deep level is twice that of the 0.20 ev level. Also the total of the two introduction rates is equal to that of the $E_v + 0.3\text{ev}$ level in crucible silicon.

It has previously been suggested that the Si-K center and the $E_v + 0.3\text{ev}$ level are related to the same defect. The currently proposed model of the K center is a double oxygen-double vacancy complex or a double A center.¹³ The conclusions reached here are consistent with that model. Oxygen is necessary for the production of the defect and no acceptor atoms are involved in the complex.

III. ANNEALING OF ELECTRON INDUCED ENERGY LEVELS IN SILICON

One method of determining the active recombination centers in electron irradiated silicon is to correlate the annealing behavior of silicon devices with annealing behavior of known defects. Considerable work has been done on annealing of radiation defects in silicon^{14,15,16}; however, no studies of annealing of the $E_v + 0.3\text{ev}$ level have been reported. For this reason we have studied the thermal annealing of the principal energy levels found in crucible grown silicon.

The annealing of energy levels was studied by means of Hall coefficients. The changes caused by annealing are reflected in Hall coefficient changes in the same way as irradiation effects. The procedures and instrumentation are identical to those previously described, and a small tube furnace was used for the annealing. The furnace temperature was controlled to within 1°C of the desired temperature, and during annealing was evacuated with a fore pump to a pressure of less than 10 microns. At higher temperatures, thermal damage to the electrical contacts on the specimen occurred, necessitating application of new contacts between annealing cycles.

The annealing data for an isochronal study of 1 ohm-cm n-type crucible silicon is shown in Figure 7. After irradiation, evidence of two energy levels is detected. The single acceptor level at $E_c - 0.17\text{ev}$ is clearly evident. There is also evidence of a deeper level which is probably the $E_c - 0.4\text{ev}$ level. The period of the isochronal anneals was 15 minutes. The effect of the first anneal at 200°C displaced the Hall

coefficient curve vertically without changing the shape. The annealing of the deeper level at $E_c - 0.4\text{ev}$ is the cause of this shift. The anneals at higher temperatures cause the low temperature end of the Hall coefficient curve to move higher while the high temperature values change only a relatively small amount indicating annealing of the $E_c - 0.17\text{ev}$ level. In this sample, the 0.17 ev level has been half annealed at 350°C and fully annealed at 400°C . The data is summarized differently in Figure 8. The vertical axis is the fraction of total radiation defects remaining in the sample. The fraction lost between room temperature and 200°C is due to the 0.4 ev level (Si-E centers). A small fraction of those levels anneal at 250°C and no further annealing was observed until 300°C is exceeded. All of the defects anneal at 400°C and the sample has returned to the unirradiated condition. Also shown on Figure 8 is a single point from the 300°C anneal of a similar specimen with a higher resistivity and correspondingly lower electron flux. This sample appears to anneal at a 50°C lower temperature.

The data on annealing of the $E_v + 0.3\text{ev}$ is summarized in Figures 9 through 12. The first attempts to anneal the 0.3 ev level were done on low dislocation crucible grown crystals. Figures 9 and 10 are typical of these efforts. It is apparent that very little annealing occurs below 400°C . Rapid annealing occurs around 500°C , with complete annealing at 550° to 600°C . These temperatures are considerably higher than those reported for n/p solar cells. For this reason additional experiments were done to determine the effect of dislocations on the annealing temperature. Figures 11 and 12 summarize this data. The material used

had dislocation etch pit densities of approximately $10^4/\text{cm}^2$. The data indicates that in the presence of high concentrations of dislocations the 0.3 ev level anneals in two stages. Roughly half of the defects anneal between 350° and 400°C . The remainder anneal between 550° and 600°C .

Previous investigations have been made of the $E_c - 0.4\text{ev}$ level (E center)^{16,17} and of the $E_c - 0.17\text{ev}$ (A center)^{15,17}. The results reported here appear to be in good agreement with these references. In general, it can be concluded that the $E_c - 0.4\text{ev}$ anneals rapidly above 100°C . The $E_c - 0.17\text{ev}$ level anneals rapidly above the 300° to 350°C range.

The annealing of the $E_v + 0.3\text{ev}$ proceeds rapidly in the 500° to 600°C range in dislocation free silicon. In highly dislocated silicon, a large fraction of the 0.3 ev level defects anneal at 400°C . The remaining defects anneal in a second stage at 550°C . It has been reported that n/p solar cells anneal rapidly in the 400°C range.¹⁸ In general a solar cell contains a large number of structural defects in that the diffusion process introduces large concentrations of dislocations. It has not been possible to isolate all of the factors affecting the 0.3 ev level annealing. It would be desirable to know what conditions will enhance the first stage annealing. If all the defects could be annealed at 400°C , it would be additional evidence of the 0.3 ev level controlling recombination in irradiated n/p solar cells.

IV. THERMAL ANNEALING OF ELECTRON IRRADIATED SOLAR CELLS

Although annealing studies have been done on some silicon devices, only recently has a comprehensive study of annealing of radiation damage in solar cells been reported.¹⁸ Until recently, commercial solar cells were very badly degraded by thermal treatments above 300°C. Some solar cells are now available with contacts which are not degraded by temperatures of 450°C and in some cases 600°C. The annealing studies of solar cells are useful for two reasons. The annealing temperatures are of practical importance to anyone designing a system to thermally remove radiation damage. Secondly, the kinetics of the annealing can be of value in identifying recombination centers and understanding the basic processes involved in disassociation of the defects.

The experimental work was performed on contemporary commercially available n/p solar cells. Cells manufactured by Hoffman, R.C.A., and Texas Instruments were irradiated and annealed. Most of the work involved isochronal annealing of irradiated cells; however, some isothermal annealing was done. The irradiations were performed with 1 Mev electrons, while the anneals were accomplished in the electronically controlled vacuum tube furnace described in the previous section. The cells were evaluated under one sun equivalent of 2800° tungsten illumination and the short circuit current was used for damage evaluation. To eliminate initial differences between cells the various parameters used to describe cell condition are as follows:

$$\% \text{ Damage Remaining} = (1 - \frac{I}{I_0}) 100$$

I = short circuit current

I_0 = short circuit current before irradiation

$$\text{Radiation Damage Remaining, Normalized} = \frac{I_0 - I_a}{I_0 - I_r}$$

I_a = short circuit current after anneal

I_r = short circuit current after irradiation

I_0 = short circuit current before irradiation

Figure 13 is a plot of damage versus isochronal annealing temperature for several electron fluxes for an annealing period of 15 minutes. The temperatures were spaced so that for any anneal, the previous lower temperature anneals represent an insignificant thermal history. The most significant pattern is the beginning of rapid anneal at 400°C. The annealing of this particular group of cells was discontinued at 450°C because significant thermal damage was found in unirradiated cells treated at 500°C. No conclusions can be reached regarding the possibility of complete annealing with these cells; however, some lightly irradiated cells were annealed to only one percent damage remaining. Some samples show a small portion of the damage annealing below 200°C which may be due to the presence of different defects such as the $E_c - 0.4\text{ev}$ level. It is interesting to note that not all samples exhibit this effect. A very minor reverse anneal is also noted at 300°C on a few samples.

Figure 14 shows similar data for a group of R.C.A. n/p solar cells. Although there are several minor differences between these cells and the previous group of Hoffman cells, the commencement of rapid annealing

is again at 400°C . These cells also show a low temperature component of the damage annealing at 100°C and strong reverse anneal in the 200°C to 300°C range. The reasons for these changes are not clear however, they seem to be in agreement with results reported by Fang¹⁸ for the same type cells. Higher temperature anneals were included to investigate the possibility of complete radiation damage annealing. The samples with lower electron fluxes have less than one percent damage remaining after anneal at 500°C . When irradiated cells were annealed at 600°C , their electrical outputs were superior to the unirradiated condition. To further investigate this effect, an unirradiated cell was heated for 15 minutes at 600°C followed by a rapid air quench. The voltage-current of this cell is shown in Figure 15. The heat treatment of the R.C.A. cell as received resulted in a significant increase in short circuit current, open circuit voltage, and maximum power output. On the basis of this result, it appears that the improved characteristics found in irradiated cells annealed at 600°C are not due to a radiation effect, but rather to a thermal effect in the cell as manufactured.

An isochronal anneal was also made on Texas Instruments cells. These cells are of considerable interest because they are fabricated from silicon with a relatively low oxygen concentration. The results of annealing for the T.I. cells are shown in Figure 16. The isochronal annealing data is very similar to that for the R.C.A. cells. The temperature for rapid annealing in the T.I. cells is slightly higher than 400°C and the last remaining damage tends to persist in the 500°C to 600°C range.

It was also observed that the T.I. low oxygen cells had the same degradation coefficient as the previous groups of 100-cm n/p cells. It can be concluded that n/p solar cells with an oxygen concentration ranging from 10^{15} to $10^{18}/\text{cm}^3$ have similar electron damage rates and similar annealing kinetics.

A few isothermal annealing cycles were made on Hoffman cells. These results are shown in Figure 17. This data is ok on a semilog plot in Figure 18. The semilogarithmic plot is a check for first order kinetics. The latter portions of the isothermal anneal appear to fit a straight line in Figure 18. The early portions of the anneals are obviously not first order. By fitting the first order equation $C/C_0 = \exp(-t/\tau)$ to the straightline portion, the reaction constant τ can be determined. In Figure 19 an Arrhenius plot is shown for the isothermal data. The activation energy indicated is 1.7ev and the pre-exponential factor is 10^{13} min^{-1} . The previous studies of radiation damage have indicated activation energies of 0.9ev to 1.5ev.^{14,16,19} In general there is not enough data presented here to conclusively prove the first order relationship. Considerable more study is necessary to support such a conclusion.

The annealing temperatures for electron irradiated n/p cells appear to be higher than those found for the $E_v - 0.17\text{ev}$ level or Si-A center. Although the annealing of the $E_v + 0.3\text{ev}$ level is still not completely understood, it has been shown that a large fraction of the 0.3ev level defects can anneal at 400°C . It is therefore possible that the large annealing effect seen in irradiated n/p cells is due to loss of the $E_v + 0.3\text{ev}$ level. Recent studies of the annealing of the Si-K center are in good agreement with this theory.²⁰

V. ELECTRON IRRADIATION OF FLOAT ZONE n-TYPE SILICON

Studies of defect introduction rates in electron irradiated float zone silicon have recently yielded interesting results. Saito and Harata¹⁶ have shown that the introduction rates for the $E_c - 0.4\text{eV}$ level (phosphorus-vacancy pair) is proportional to the concentration of phosphorus in the sample. In another study, Stein²¹ reported that for electron irradiation of float zone silicon the removal rate changes very little in the phosphorus concentration range of 10^{14} to $10^{16}/\text{cm}^3$. To clarify these results, several Hall samples of float zone n-type silicon were irradiated with 1 MeV electrons. The silicon crystals were grown by TRW-Semiconductors with phosphorus concentrations ranging from 10^{15} to $10^{18}/\text{cm}^3$. The Hall coefficient was measured before and after irradiation.

In Figure 20 the defect introduction rate is plotted versus the carrier concentrations for the various samples irradiated. The introduction rate includes all energy levels above the position of the Fermi level at liquid nitrogen temperature. This limitation includes all the commonly known energy levels in n-type silicon. When several points are shown for the same sample, such as the 0.23 and 0.67 Ω -cm samples, the data shows the reduction in introduction rate with remaining carrier concentration after repeated electron irradiation. The arrows indicate the trend for increasing electron exposure. The total introduction rate is seen to rise very slowly through three orders of magnitude charge carrier or phosphorus concentration. The slope of this variation is identical to that reported by Stein, but the values are a factor of two lower. In

case of the 6.8 Ω -cm sample, it was possible to separate the introduction rate of the $E_c - 0.4\text{ev}$ and the $E_c - 0.17\text{ev}$ levels. The total introduction rate was 0.6 cm^{-1} . The introduction rate for the $E_c - 0.4\text{ev}$ level was 0.25 cm^{-1} , in good agreement with that reported by Saito and Harata.¹⁶

The linear relationship between introduction rate of the $E_c - 0.4\text{ev}$ level and the phosphorus concentration reported by Saito and Harata obviously does not extend to phosphorus concentrations greater than $10^{16}/\text{cm}^3$. It is likely that the displacement production rate of approximately 2 cm^{-1} will restrict the introduction rates for defects to lower values. The linear decrease in defect introduction rate with remaining carrier concentration is probably evidence of phosphorus-vacancy pair production.

The Hall coefficient data for irradiation of the 0.023 Ω -cm sample is shown in Figure 21. The Hall coefficients have been converted into electrons/ cm^3 . Experimental difficulties necessitated a change of Hall voltage arms after the $2 \times 10^{17}\text{e}/\text{cm}^2$ irradiation, hence a slight shift is apparent in the data. The unirradiated sample indicates an activation energy very close to the conduction band edge. This sample is nearly degenerate and the phosphorus ground level energy has been lowered by wave function overlap because of the high phosphorus concentration. As the electron flux is increased, the activation energy is increased. No evidence of shallow radiation damage levels or bands of such levels is indicated.

A plot of the activation energies of the sample after various irradiations versus the donor concentration is shown in Figure 22. The data appears to fit a one-third power relationship. The equation

$$E_d = [0.044\text{ev} - 3 \times 10^{-8} (N_d)^{1/3}] \text{ev}$$

is fitted to the data. Similar equations have been presented by Pearson and Bardeen²² and Debye and Conwell²³ to describe variation of ionization energy of donor and acceptor atoms with concentration.

Further study is necessary to conclusively support the data; however, the data available does allow certain conclusions. This heavily doped silicon is in the impurity conduction or overlap state before irradiation. During the electron irradiation, the principal stable defect formed is the phosphorus-vacancy pair. The decrease in the phosphorus donors raises the ionization energy by reducing the overlap of wave functions. The previously mentioned decrease of introduction rate with increasing electron flux is additional evidence of a phosphorus defect complex forming.

VI. TEMPERATURE DEPENDENCE OF ELECTRON DAMAGE IN SOLAR CELLS

Considerable effort has been made to determine the response of silicon solar cells to energetic electron bombardment. Nearly all of this work has been on the basis of a room temperature environment for the solar cell. The range of temperatures possible in satellite operations is subject to considerable variation. Many factors enter into the decision of the space operating temperatures for solar cells. The primary considerations are the temperature variation of short circuit current, open circuit voltage, maximum power output, and optimum load line. In the presence of a radiation environment, the temperature dependence of damage rate should also be included in the considerations.

An irradiation chamber was attached to the TRW Van de Graaff in which solar cells were irradiated at temperatures between 77° and 373°K . The apparatus is shown in Figures 23 and 24. It was intended to allow alternate electron irradiation and evaluation under one sun illumination by 180° rotation of the vertical cold finger. It became immediately obvious in the course of the experiments that extraction of the temperature dependence of the damage coefficient from the I-V characteristics in the presence of the many other temperature dependences already present in the I-V characteristic would be a complex task with only limited creditability. Since the principal objective was to determine the temperature dependence of the introduction rate of active recombination centers, the use of I-V characteristics was discarded in favor of measurements of minority carrier diffusion length. The experimental

procedure used therefore was to irradiate the cells with 1 MeV electrons and then evaluate the damage at the irradiation temperature by measuring the diffusion length. The electron beam currents were monitored by calibration of the current intercepted by a 0.001" aluminum foil in the beam. The diffusion lengths were measured by a modified Gremmelmaier technique.²⁴ In this measurement, the short circuit produced in the cell by a low flux of 1 Mev electrons is determined. The damage constant is defined as follows:

$$\frac{1}{L^2} = \frac{1}{L_0^2} + K\phi$$

L = diffusion length after irradiation

L₀ = diffusion length before irradiation

φ = electron flux

K = damage constant.

The parameter most directly related to the introduction rate of active recombination centers is the minority carrier lifetime. Since both the minority carrier lifetime and the diffusion coefficient D are temperature dependent, the measurement of minority carrier diffusion length has to be adjusted in order to yield data dependent only on temperature dependence of the defect introduction rate. To accomplish this adjustment, the diffusion length of each cell was first read at room temperature in the experimental configuration. The desired experimental temperature was then obtained and prior to the first irradiation step the diffusion length excitation flux was adjusted to yield the same diffusion length current as previously obtained at room temperature. This electron flux was then

used through the remainder of the experiments at that particular temperature for the measurement of diffusion length degradation. Diffusion length was then measured as a function of integrated flux to confirm the $-\frac{1}{2}$ slope required for the use of the damage coefficient K as given in the above equation. At all temperatures the cells exhibited a $-\frac{1}{2}$ slope of diffusion length versus integrated flux. At the completion of each series of exposures the test cell was returned to room temperature and the diffusion length was again measured with the standard excitation flux. In all cases the room temperature diffusion length readings agreed with those obtained at the completion of the exposure at the test temperature. All cells of each given type were irradiated to the same integrated flux after which the cells were evaluated under one sun illumination. Solar cells of both polarity, manufactured by Hoffman, were evaluated. Sample temperatures were monitored by thermocouple during irradiation and remained constant within 2°C during irradiation.

The experimental values of K, the damage rate, are plotted as a function of irradiation temperature in Figure 25. Data for both polarity cells are shown. The results indicate that between 77° and 300°K the damage rate for p/n solar cells remains essentially constant. The damage rate for n/p cells was constant between 198° and 373°K, but increased by a factor of 5 at 77°K. The room temperature evaluation of these cells is shown in Figure 26. The room temperature short circuit current density of all cells after irradiation is independent of the irradiation temperature.

Several conclusions can be drawn from these data. First, electrical characteristics of irradiated cells of both polarities are identical at room temperature regardless of irradiation temperature from 77° to 373°K. Secondly, the damage coefficient K of both p/n and n/p cells is independent of the radiation temperature over this temperature range with the single exception of n/p solar cells at 77°K. Since the room temperature data of n/p cells irradiated at 77°K are virtually identical with other n/p cells irradiated at different temperature, several possibilities for this one exception exist; (1) the dominant recombination center at 77°K in p-type silicon may be a different defect energy level than at higher temperatures or (2) the defects introduced at 77°K may be of a different species which upon raising to a higher temperature form the stable defect sites normally observed. In any event, it is interesting to note that the damage coefficient for minority carrier lifetime in p-type silicon is actually higher by a factor of 5 as opposed to more conventional situations wherein irradiation at lower temperatures, if anything, usually inhibits the migration and formation of active defect sites. For example, Wertheim²⁵ and Novak²⁶ have made studies of electron damage in silicon as a function of temperature. Their investigations relate to specific energy levels or carrier removal sites in irradiated silicon and they reported large decreases in damage rates for irradiations below 200°K. Since previous measurements of minority carrier lifetime versus temperature in p-type silicon indicate no irregularities at 77°K, it appears likely that an extremely active recombination center energy level exists which can only be produced and observed at temperatures of 77°K or lower. It is also apparent that the low temperature recombination center once formed is not stable at higher temperatures.

VII. RECOMBINATION CENTERS IN ELECTRON IRRADIATED SOLAR CELLS

The present state of knowledge regarding recombination centers in electron irradiated silicon is far from satisfactory. The conclusions reached by different investigations appear to be very much in conflict.¹⁻⁵ A summary of results reported is shown in Table 1. Several conflicts are apparent regarding the defect level for irradiated silicon of both types. The correct understanding of the recombination center is basic to any knowledge of electron damage in silicon. For this reason, a study was done to repeat recombination work previously done in this laboratory for confirmation purposes and extend it to p/n solar cells.⁵ The basic principle of this technique is measurement of diffusion length of solar cells as a function of temperature. The minority carrier lifetime can be calculated from the experimental diffusion length and analyzed in terms of recombination theory.^{27,28}

For the case of recombination of small excesses of minority carriers through small concentrations of defect centers in n-type silicon, the lifetime will obey the following expression:

$$(A) \quad \tau = \tau_{p0} \left(1 + \frac{n_1}{n_0} \right)$$

if the recombination level is in the upper half of the band gap. If the recombination level is in the lower half of the band gap the expression

$$(B) \quad \tau = \tau_{p0} \left(1 + \frac{\tau_{n0}}{\tau_{p0}} \frac{p_1}{n_0} \right)$$

will describe the minority carrier lifetime. The various symbols are

used in the same manner as the original reference.²⁸ A similar set of equations can be written for recombination in p-type silicon.

The experimental details have been described in previous reports.⁵ A solar cell is mounted with scattering foil in a variable temperature dewar. Under a low 1 Mev electron flux, the solar cell short circuit current is calibrated to indicate diffusion length. The mobility data of Ludwig and Watters²⁹ is used to convert the diffusion length to minority carrier lifetime. The solar cells used were manufactured by Hoffman Electronics.

The results of the study of both p/n and n/p solar cells are shown in Figures 27 through 30. Data is shown for both unirradiated and electron irradiated cells. The determination of the recombination center involves fitting the experimental points to the theoretical equations of the statistics of recombination. As previously mentioned one of two equations will describe the lifetime, depending on the location of the energy level of the recombination center. The problems involved in fitting these curves are well illustrated in Figure 27. This figure shows the data for an unirradiated p/n solar cell. An attempt has been made to make the best possible fit for both equations. In this case, neither fit is perfect; however, one can examine the accuracy of the possible conclusions more carefully. Equation (B) contains three variables (τ_{p0} , τ_{n0} , P_1), while equation (A) contains only two variables (τ_{p0} , n_1). The probability of achieving a better fit of an equation to a

set of experimental points rises very fast with the number of variables in the equation. For this reason, conclusions resulting from fits of equation (B) to experimental data are subject to question. It is simply too easy to avoid unaccounted factors such as temperature dependence of τ_{p_0} or τ_{n_0} by using equation (B) rather than (A). Also, in the case of Figure 27 the use of equation (B) requires the assumption that $\tau_{n_0}/\tau_{p_0} = 1$. This restriction is undesirable because it implies that the recombination center is uncharged at all times. Despite the poor fit of equation (A), one might conclude that the data indicates that a level near $E_c - 0.17\text{ev}$ controls recombination in unirradiated p/n solar cells. In any event an energy level in the 0.15 ev to 0.17 ev range is evident.

The analysis of an irradiated p/n solar cell is shown in Figure 28. This cell was irradiated with 1×10^{14} e/cm², 1 MeV electrons. In this case equation (A) can be fitted to the data. The recombination center level is at $E_c - 0.17\text{ev}$. At low temperatures, the data points do not fit the theoretical curve; however, there is good reason for reduced accuracy in the experimental lifetimes at low temperatures. The lifetime values are calculated from the measured diffusion length values by this equation:

$$(C) \quad \tau = \frac{L^2}{D}$$

where L = diffusion length

τ = minority carrier lifetime

D = diffusion constant.

The diffusion constant is calculated from drift mobility data by this equation

$$(D) \quad D = \frac{\mu kT}{e}$$

where μ = drift mobility.

At lower temperatures the mobility is subject to more variation because of electron-impurity scattering. Thus the use of assumed mobilities at low temperatures can cause small errors. This is not likely at higher temperatures where electron-phonon scattering limits the mobility. Since the low temperature values of the diffusion constant are questionable, it is reasonable to expect a poorer fit of lifetime to theory at low temperature. Considering the use of equation (A) rather than (B), and the excellent fit to theory, the evidence is very strong for the $E_c - 0.17\text{ev}$ level (Si-A center) acting as the recombination center in p/n solar cells. This result is in excellent agreement with Galkin, et al,³ but differs with Wertheim's conclusions.²

The data for an unirradiated n/p solar cell is shown in Figure 29. It was possible to fit a theoretical curve for an acceptor level at $E_c - 0.07\text{ev}$ to the experimental points. Although the fit appears to be good, it was necessary to use the p-type equivalent of equation (B) to make the fit. For this reason, any conclusions are subject to question. This appears to be the first evidence of such an energy level in silicon.

Figure 30 illustrates the analysis for an electron irradiated n/p solar cell. In this case, it was also necessary to use the p-type equivalent of equation (B). The theoretical curve for recombination

through an acceptor level at $E_c - 0.15\text{ev}$ is fitted to the data. A previous study reported in this laboratory indicated similar results.⁵ This previous result better fitted a level at $E_c - 0.17\text{ev}$. The difference between these results is not considered significant.

The first analysis seems to indicate that the $E_c - 0.17\text{ev}$ (Si-A center) is the recombination center in the irradiated n/p solar cell. This conclusion is in direct conflict with data on annealing of irradiated cells and variation of damage rate with electron energy for n/p solar cells. These other data indicate that the electron damage recombination center in n/p cells is not the $E_c - 0.17\text{ev}$ (Si-A center), and probably is the $E_v - 0.3\text{ev}$ level (Si-K center).

A solution to this dilemma can be suggested from the model of the Si-K center recently proposed. Almeleh has suggested that the K center structure is a double A center,¹³ a complex of two vacancies and two oxygen atoms in a chain. It is proposed that the strained oxygen-oxygen bond can donate an electron to the valence band with an activation energy of 0.3 ev. Another feature of the model is two Si-Si molecular bonds formed between silicon atoms in the next to nearest neighbor positions. In the case of the A center, Watkins and Corbett have shown that such a Si-Si bond can accept an additional electron in an antibonding orbital at $E_c - 0.17\text{ev}$.⁶ If similar behavior is possible in the K center, it is reasonable to expect the K center to have a double acceptor level in the vicinity of $E_c - 0.17\text{ev}$. The coulombic interactions of such a doubly charged complex could make such a defect a potent recombination center. If interaction between the two orbitals is possible the energy level would be closer to the conduction band edge than 0.17 ev.

There has been no direct evidence of acceptor levels at $E_c - 0.17\text{ev}$ being related to the same defect as the $E_c + 0.3\text{ev}$ donor level, nor has there been any evidence of any level at $E_c - 0.17\text{ev}$ other than that of the A center, an oxygen vacancy pair. If such a level were also associated with the K center or $E_v + 0.3\text{ev}$ level defect, it would be very difficult to detect because of the low introduction rate. This would be particularly true in the presence of A centers. At present, the only way to rationalize all the various results relating to electron damage in n/p solar cells is to hypothesize recombination through an acceptor level $0.15 - 0.17\text{ ev}$ below the conduction band which is associated with the K center. The alternate is accepting the $E_c - 0.17\text{ev}$ level (A center) or $E_v + 0.3\text{ev}$ level (K center) as the recombination center and discount the conflicting evidence between the two.

Table 1

Summary of Reported Recombination Levels in Electron Irradiated Silicon

<u>Author</u>	<u>Silicon</u>	<u>Electron Irradiation</u>	<u>Defect Level</u>	<u>Method</u>	<u>Capture Cross Section</u>
Wertheim ^{1,2}	n-type	0.7 Mev	$E_V + 0.27\text{ev}$	Diode Reverse Recovery	$\sigma_p = 8.0 \times 10^{-13}\text{cm}^2$
					$\sigma_n = 9.5 \times 10^{-14}\text{cm}^2$ (Acceptor)
Galkin, et al ³	p-type	0.7 Mev	$E_C - 0.16\text{ev}$	Diode Reverse Recovery	$\sigma_p = 1.8 \times 10^{-14}\text{cm}^2$
					$\sigma_n = 1.9 \times 10^{-14}\text{cm}^2$
	n-type	1.0 Mev ($\text{Sr}^{90} - \text{Y}^{90}$)	$E_C - 0.16\text{ev}$	a.c. Diode Modulation	$\sigma_p = 4.0 \times 10^{-14}\text{cm}^2$
					$\sigma_n = 1.1 \times 10^{-15}\text{cm}^2$ (Acceptor)
Baicker ⁴	n-type (P)	0.5 - 0.7 Mev	$E_C - 0.17\text{ev}$	Pulsed Van de Graaff Injection	(Acceptor)
	n-type (As)		$E_C - 0.17\text{ev}$	"	(Acceptor)
	n-type (Sb)		$E_V + 0.27\text{ev}$	"	(Acceptor)
	p-type	0.7 Mev	$E_V + 0.18\text{ev}$	"	(Donor)
TRW ⁵	p-type	1.0 Mev	$E_C - 0.17\text{ev}$	Modified Grennelmaier	(Acceptor)
				L vs T	
				L vs P _O	

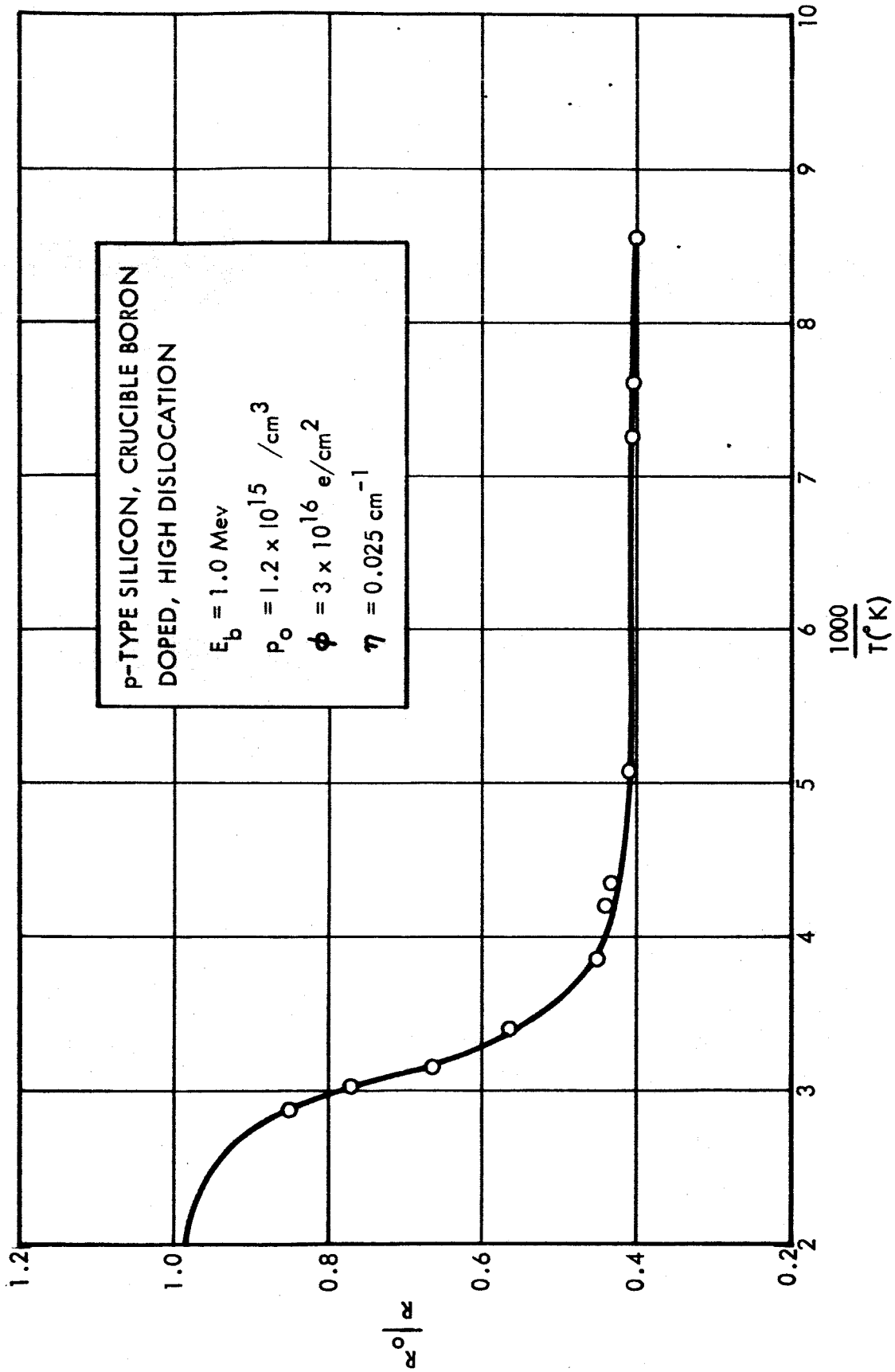


Figure 1. Hall Coefficient of Electron Irradiated Boron Doped Crucible Grown p-type Silicon

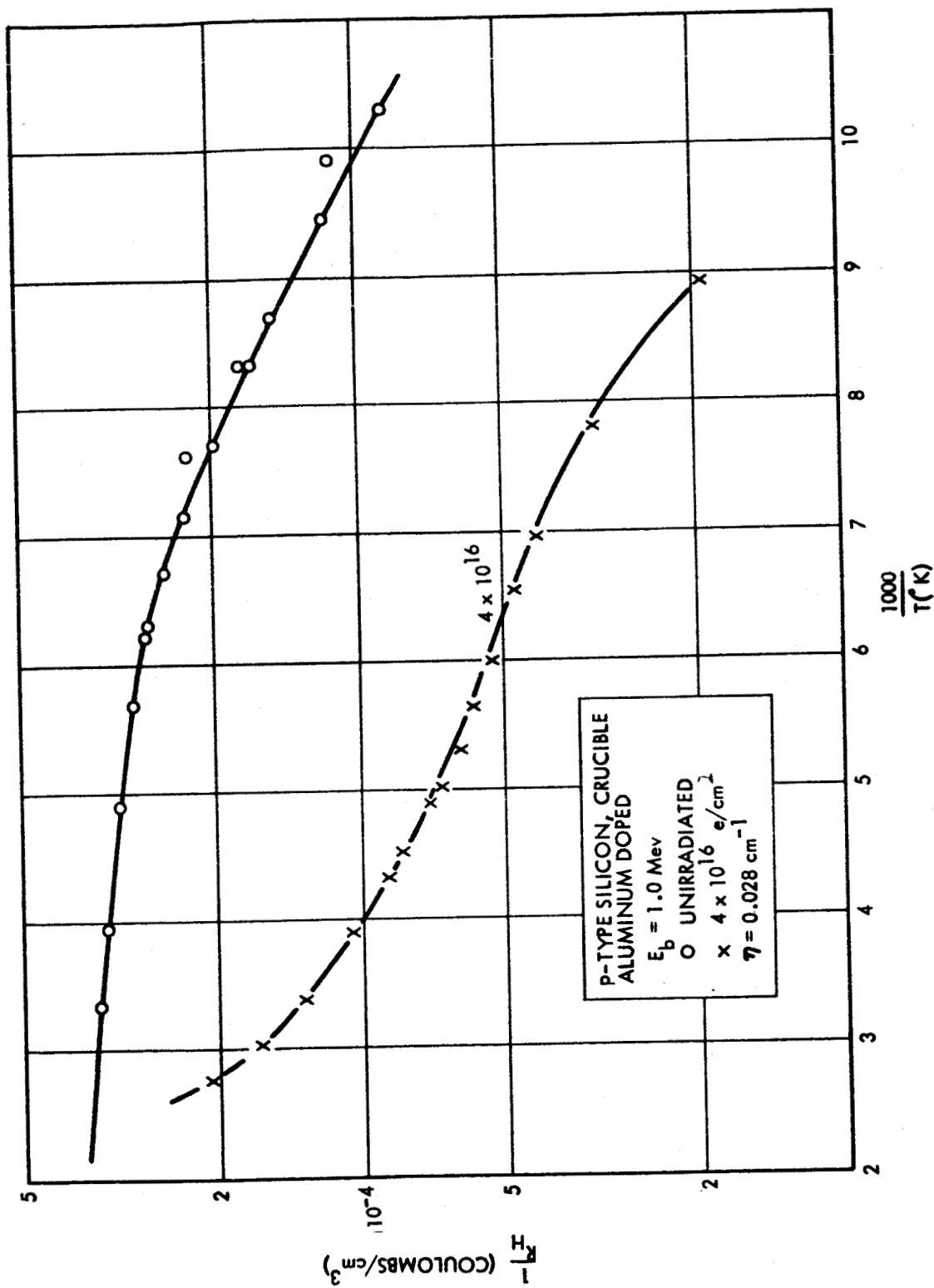


Figure 2. Hall Coefficient of Electron Irradiated Aluminum Doped Crucible Grown p-type Silicon

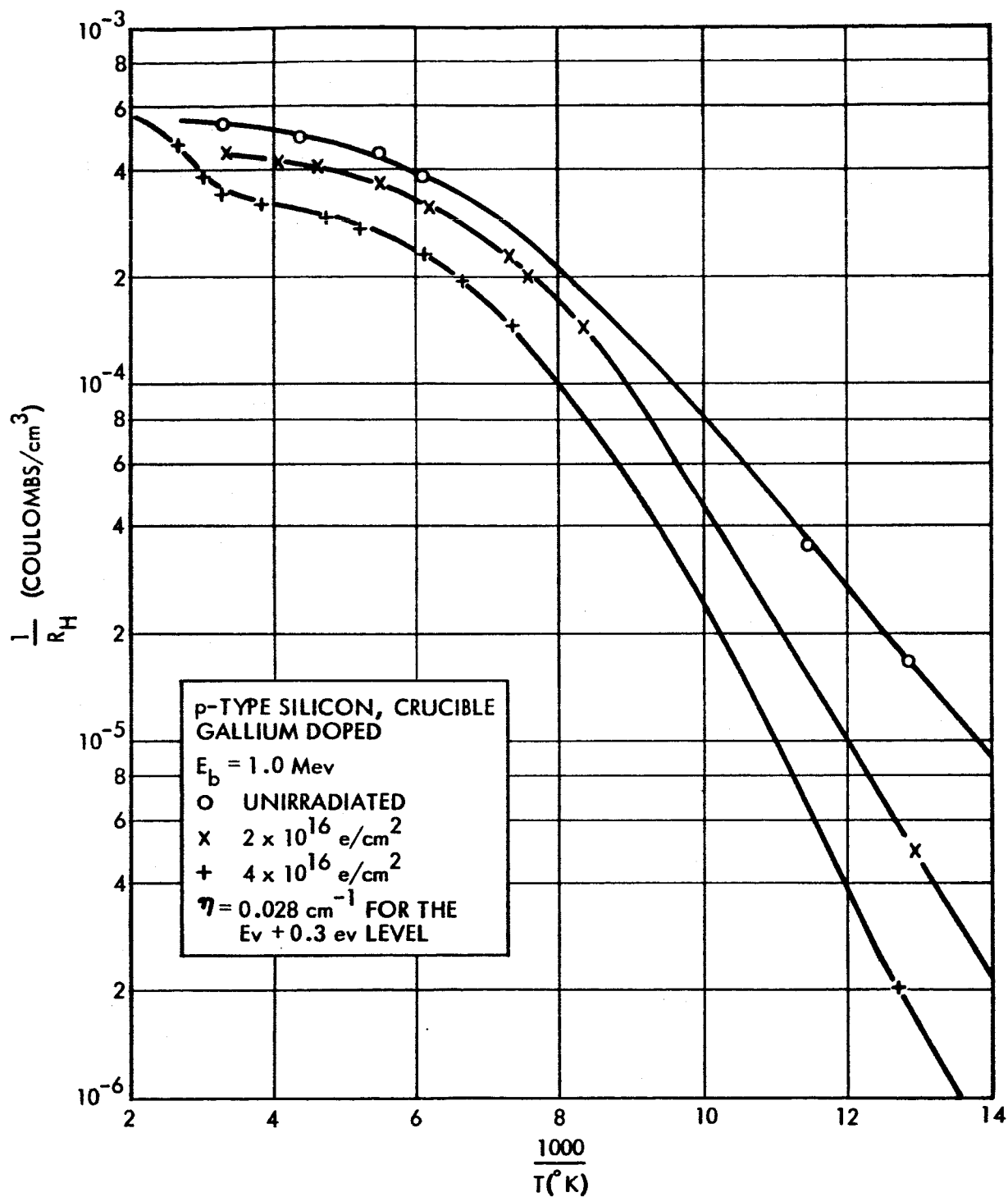


Figure 3. Hall Coefficient of Electron Irradiated Gallium Doped Crucible Grown p-type Silicon

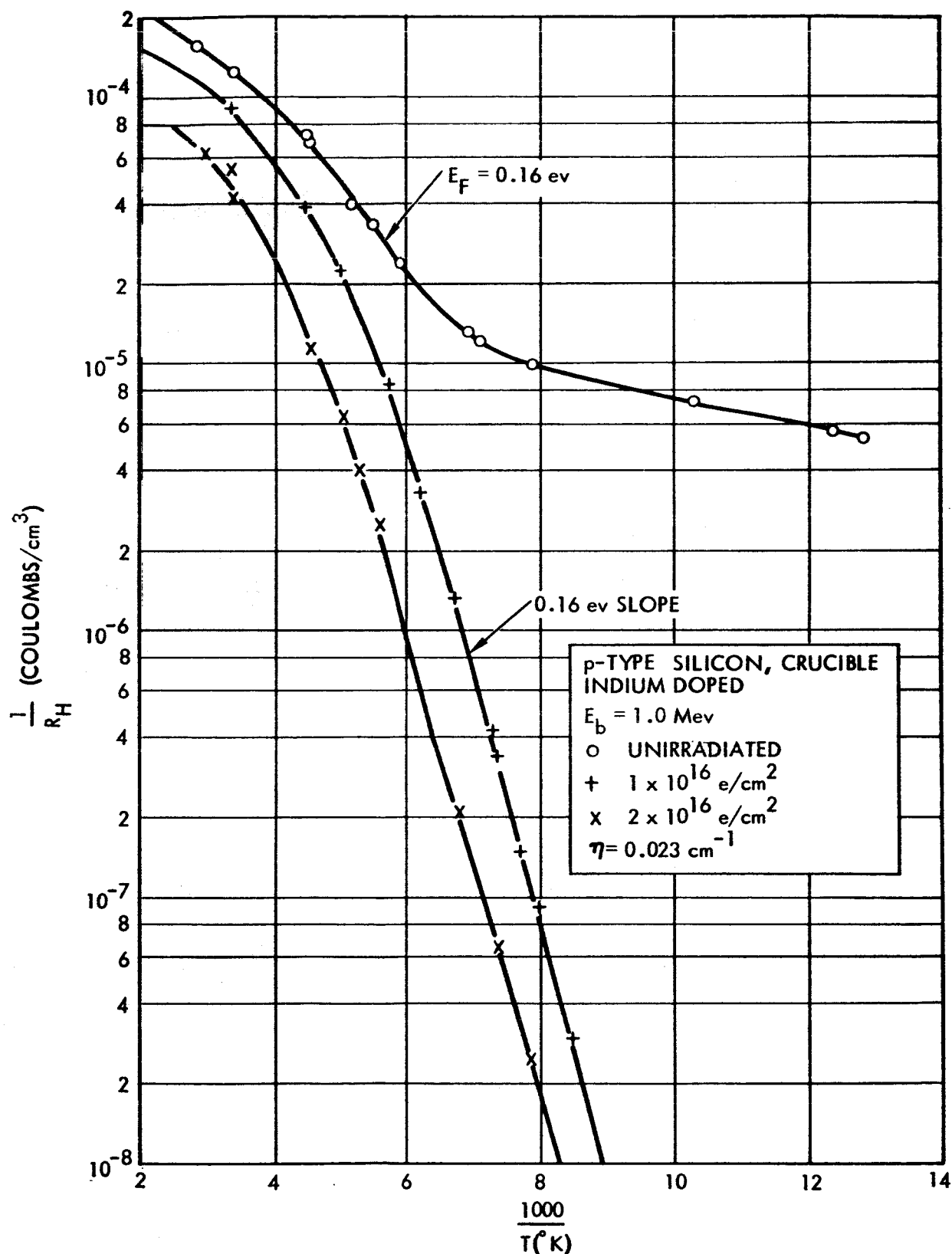


Figure 4. Hall Coefficient of Electron Irradiated Indium Doped Crucible Grown p-type Silicon

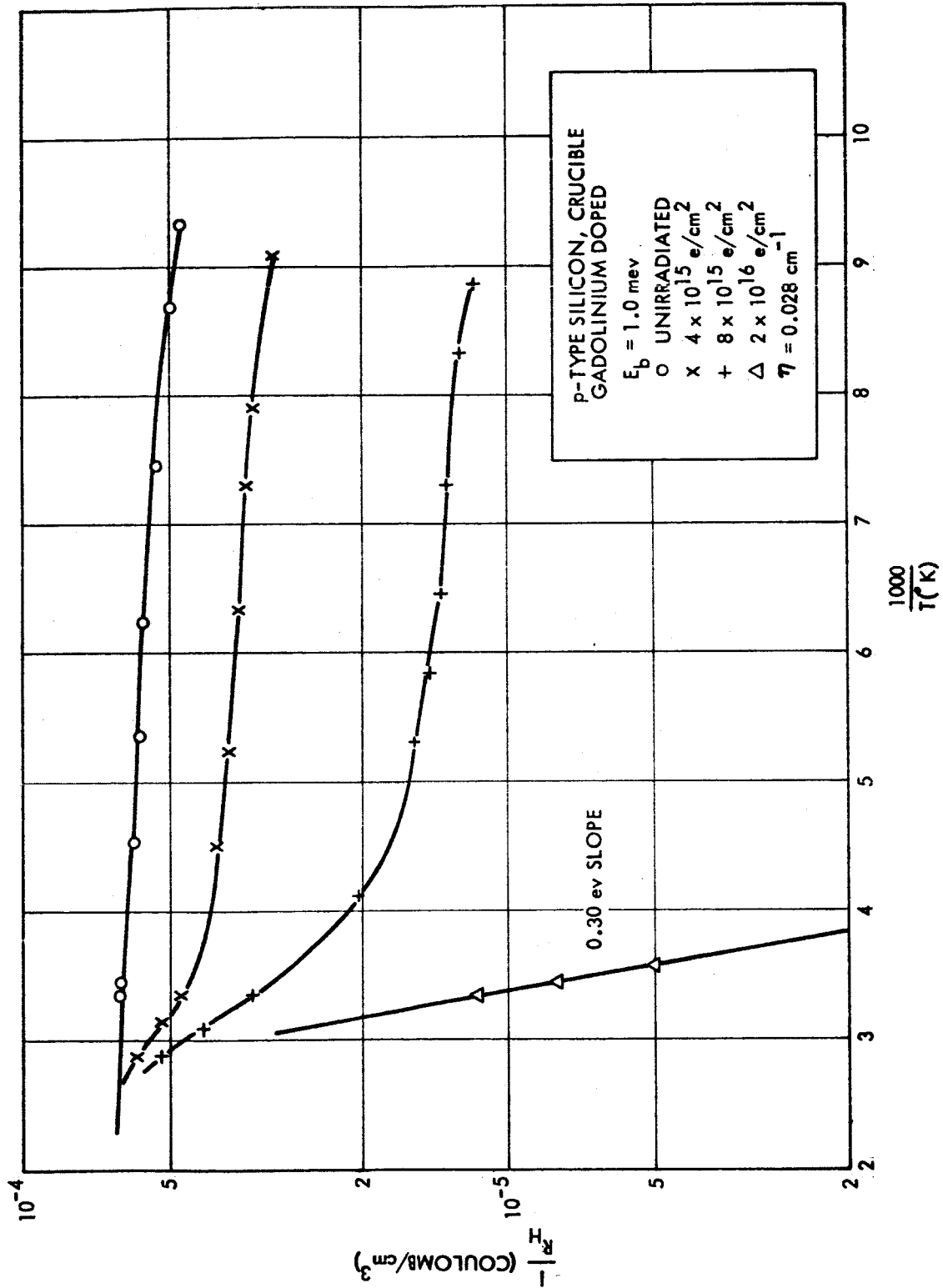


Figure 5. Hall Coefficient of Electron Irradiated Gadolinium Doped Crucible Grown p-type Silicon

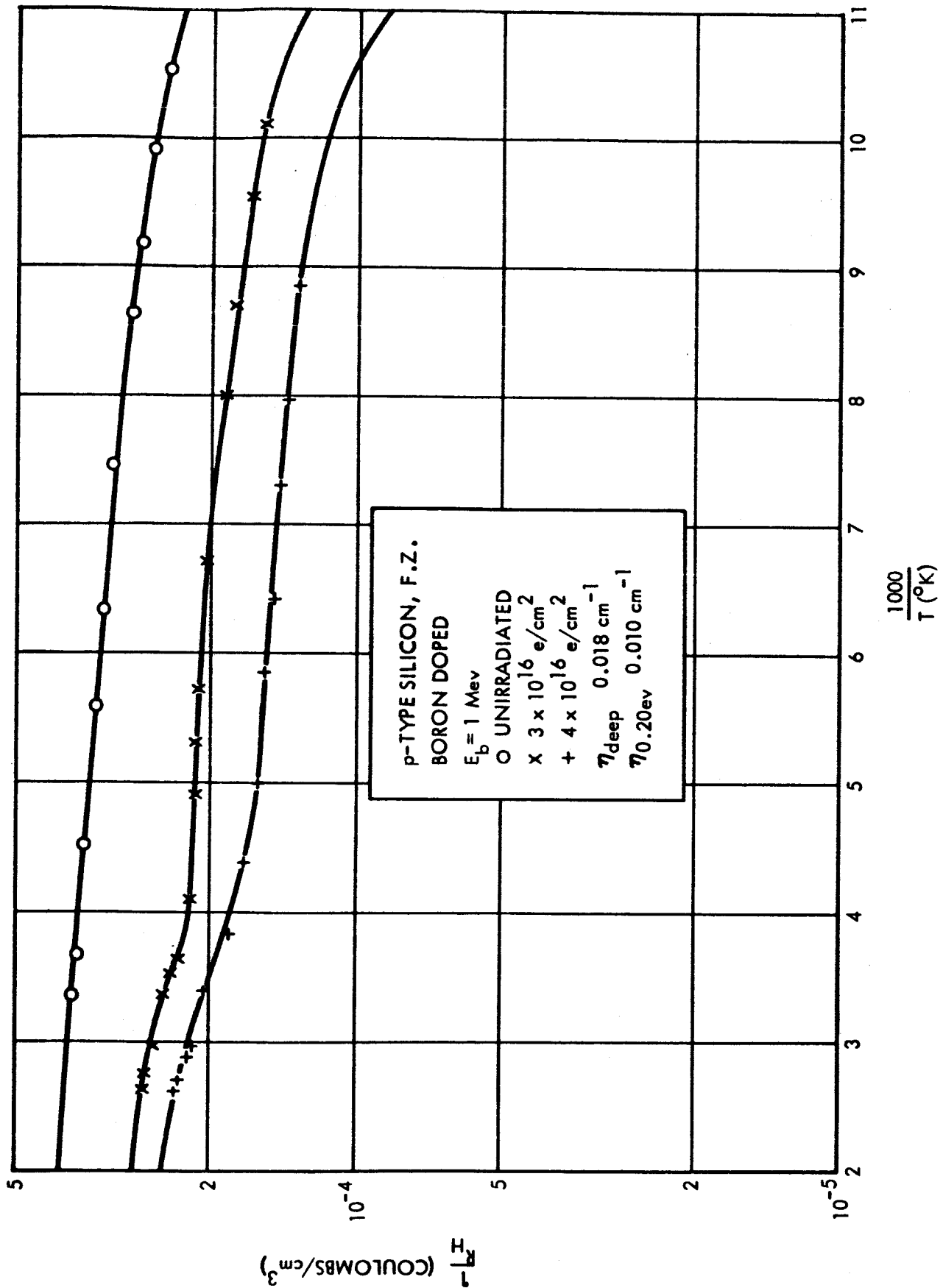


Figure 6. Hall Coefficient of Electron Irradiated Boron Doped Float Zone p-type Silicon

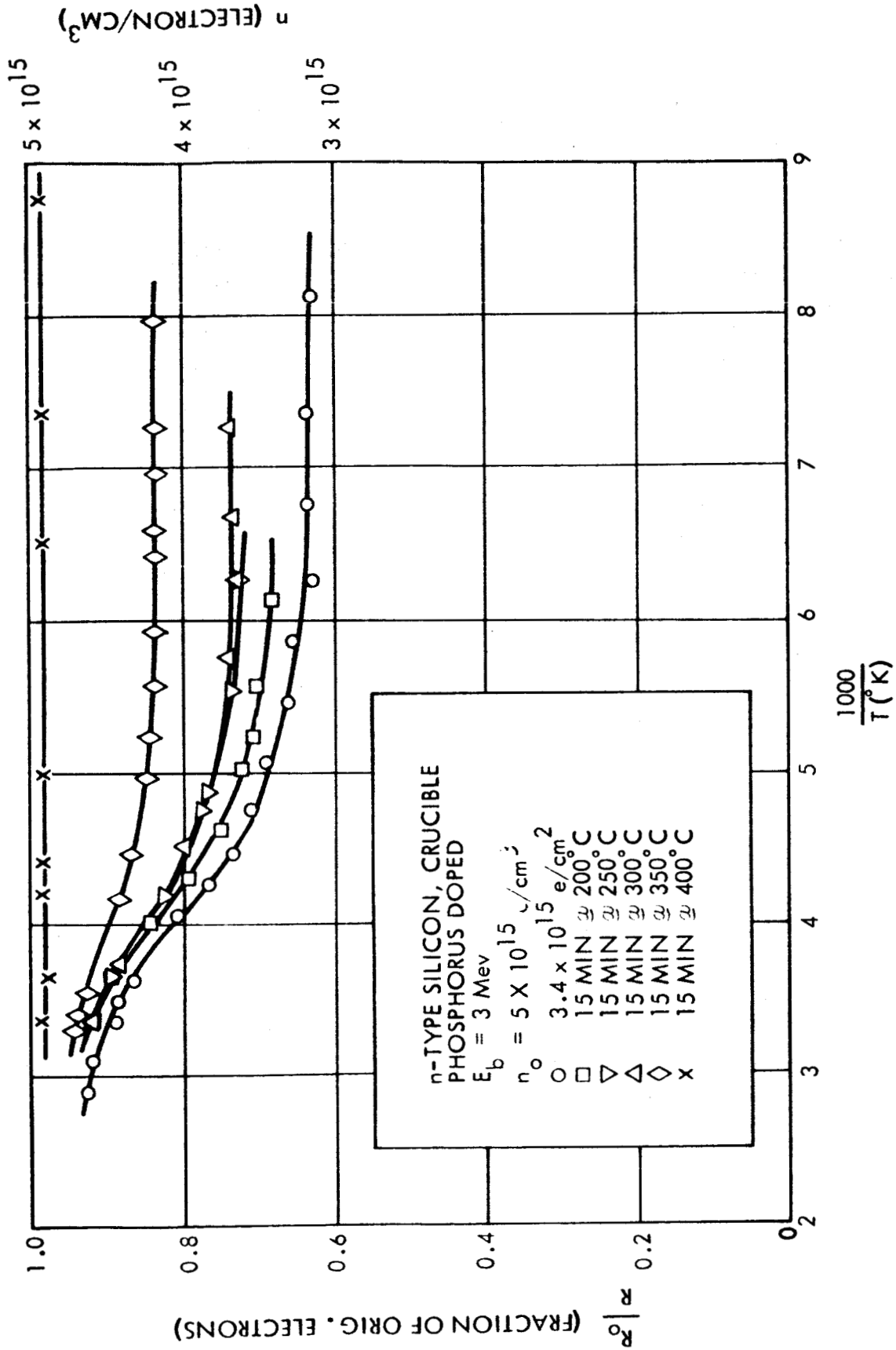


Figure 7. Hall Coefficient Data for Isochronal Annealing of
Electron Irradiated Crucible Grown n-type Silicon

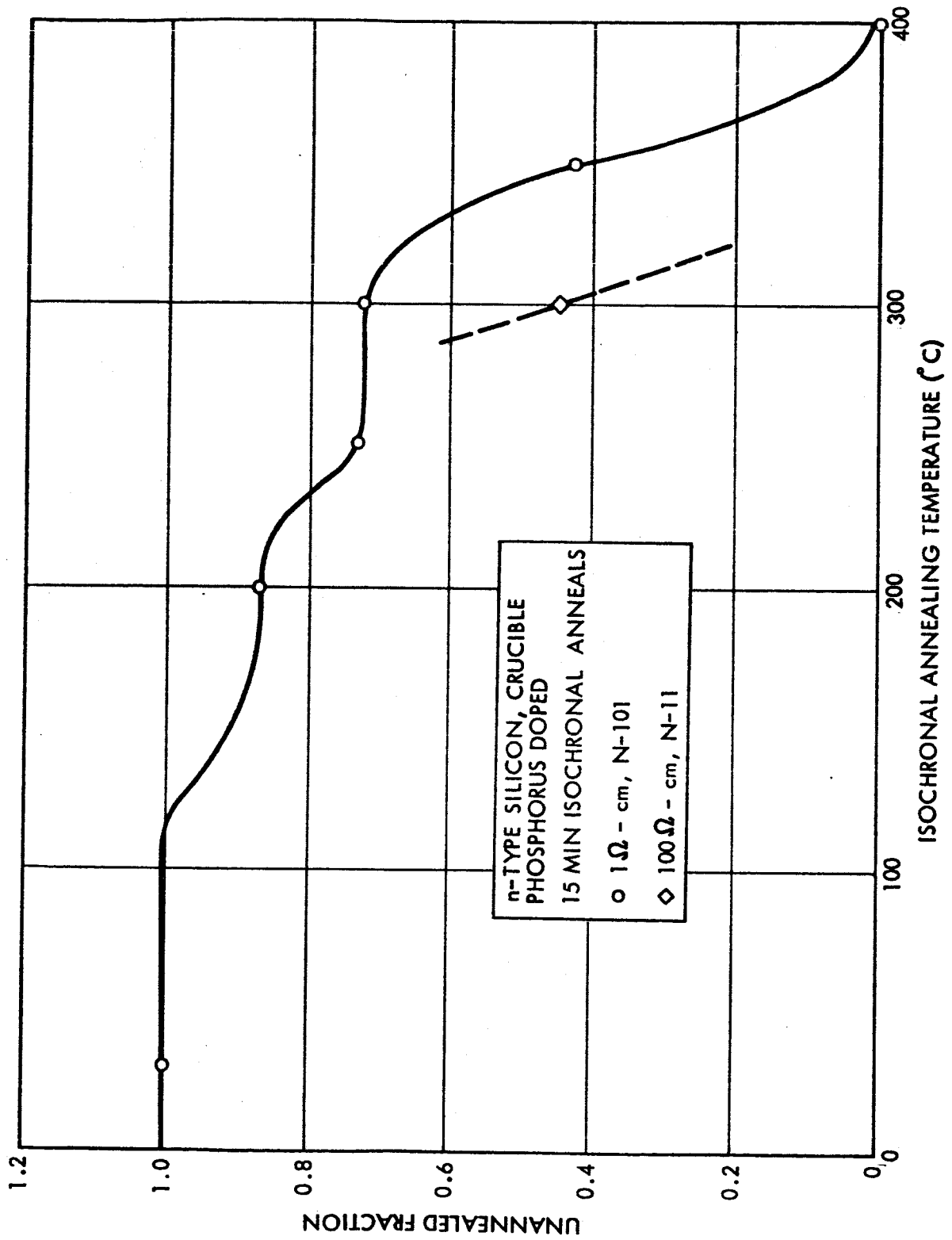


Figure 8. Isochronal Annealing of Electron Irradiated
Crucible Grown n-type Silicon

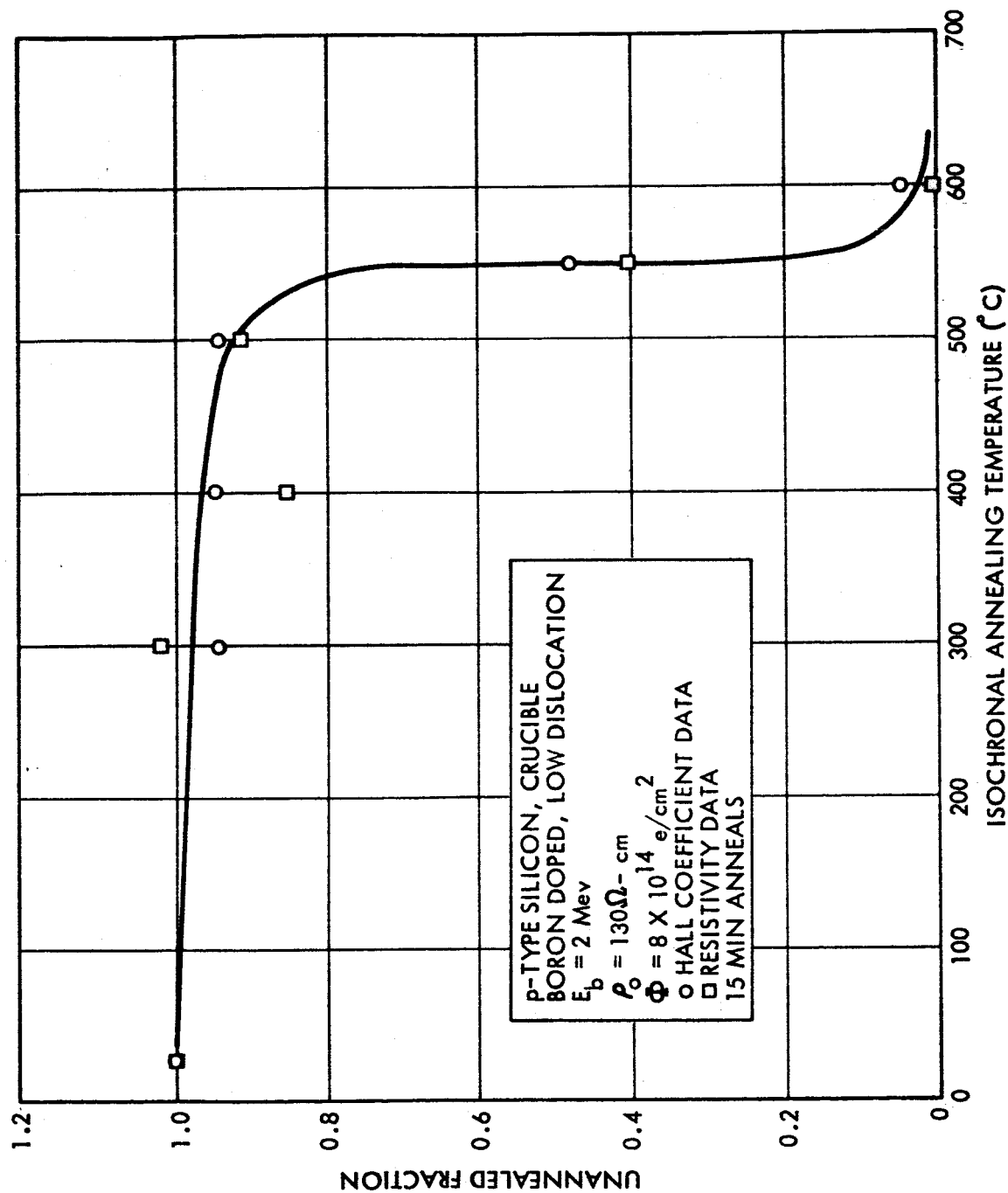


Figure 9. Isochronal Annealing of Electron Irradiated Crucible Grown p-type Silicon (130 Ω -cm, low dislocation)

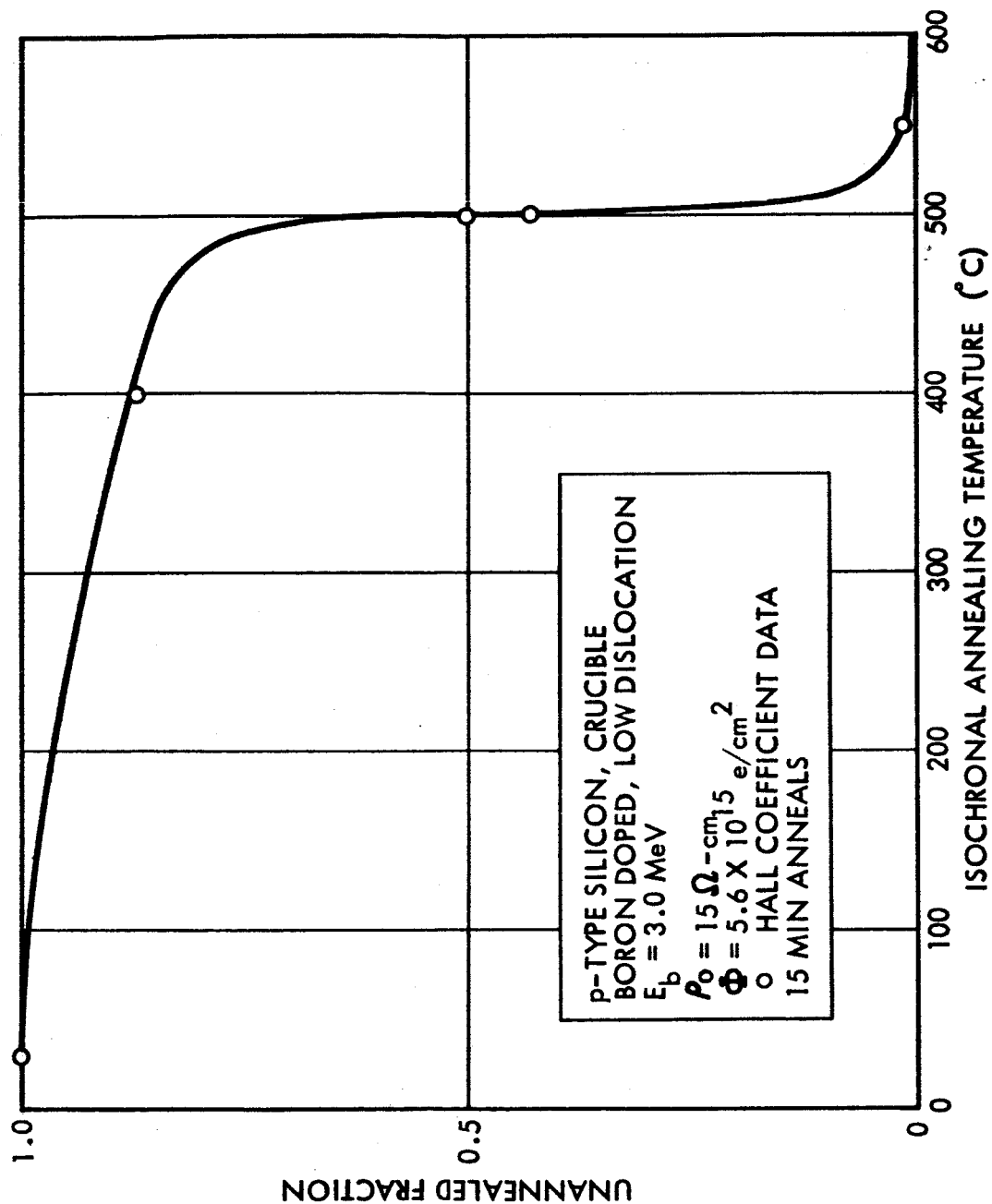


Figure 10. Isochronal Annealing of Electron Irradiated Crucible Grown p-type Silicon (15 Ω -cm, low dislocation)

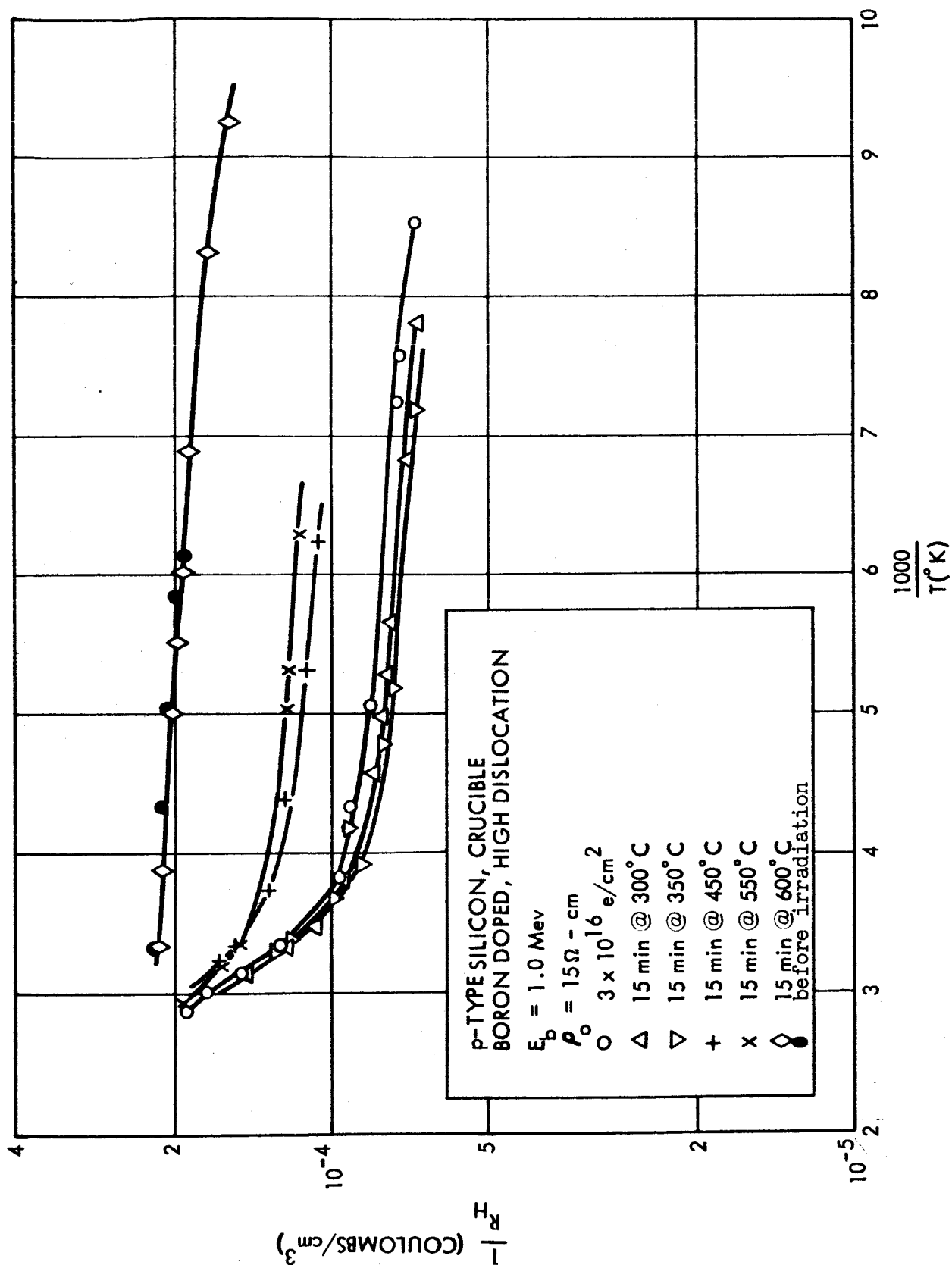


Figure 11. Hall Coefficient Data for Isochronal Annealing of Electron Irradiated, Crucible Grown p-type Silicon ($15 \Omega \cdot \text{cm}$, high dislocation)

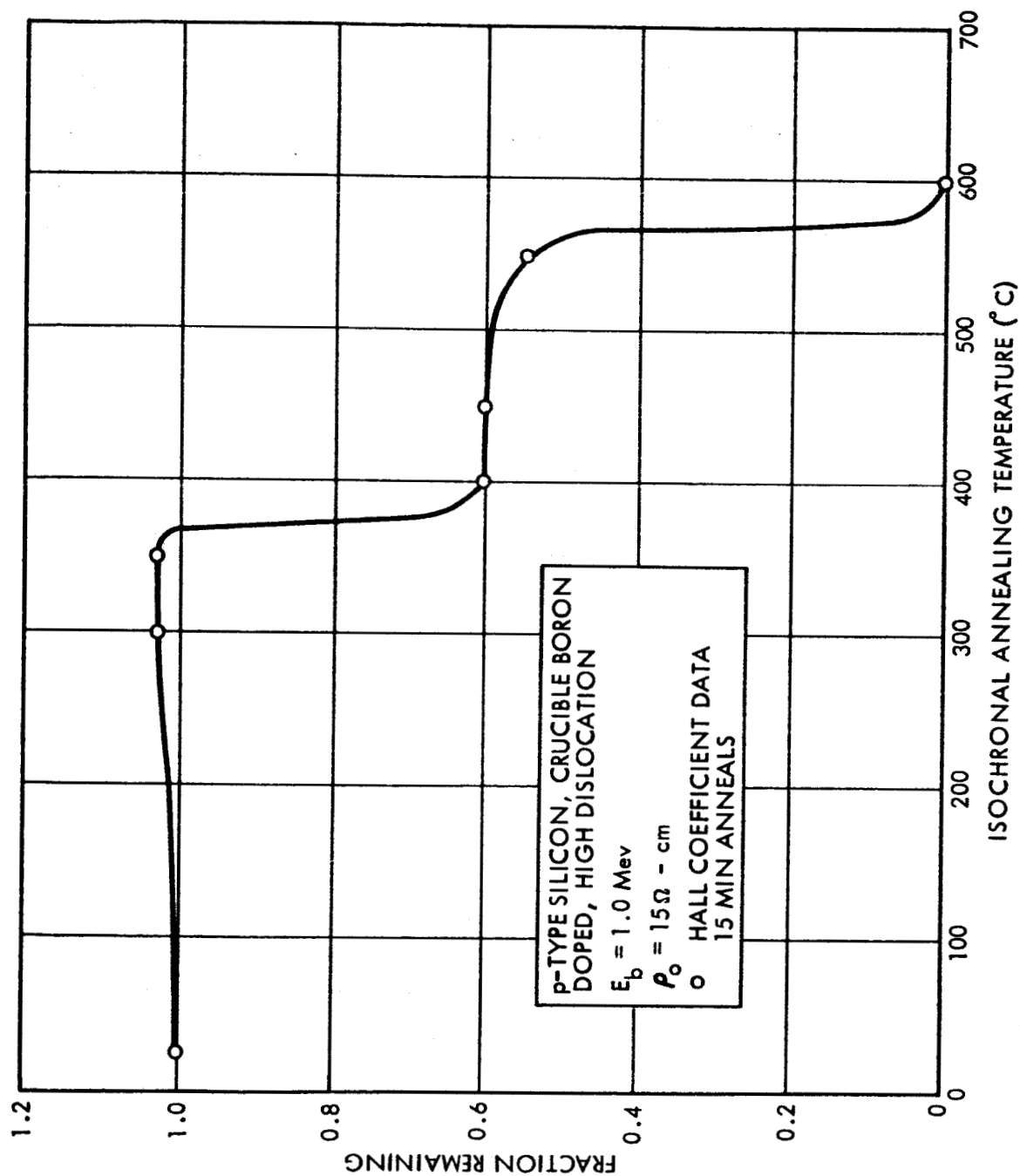


Figure 12. Isochronal Annealing of Electron Irradiated Electron,
Crucible Grown p-type Silicon ($15 \Omega \cdot \text{cm}$, high dislocation)

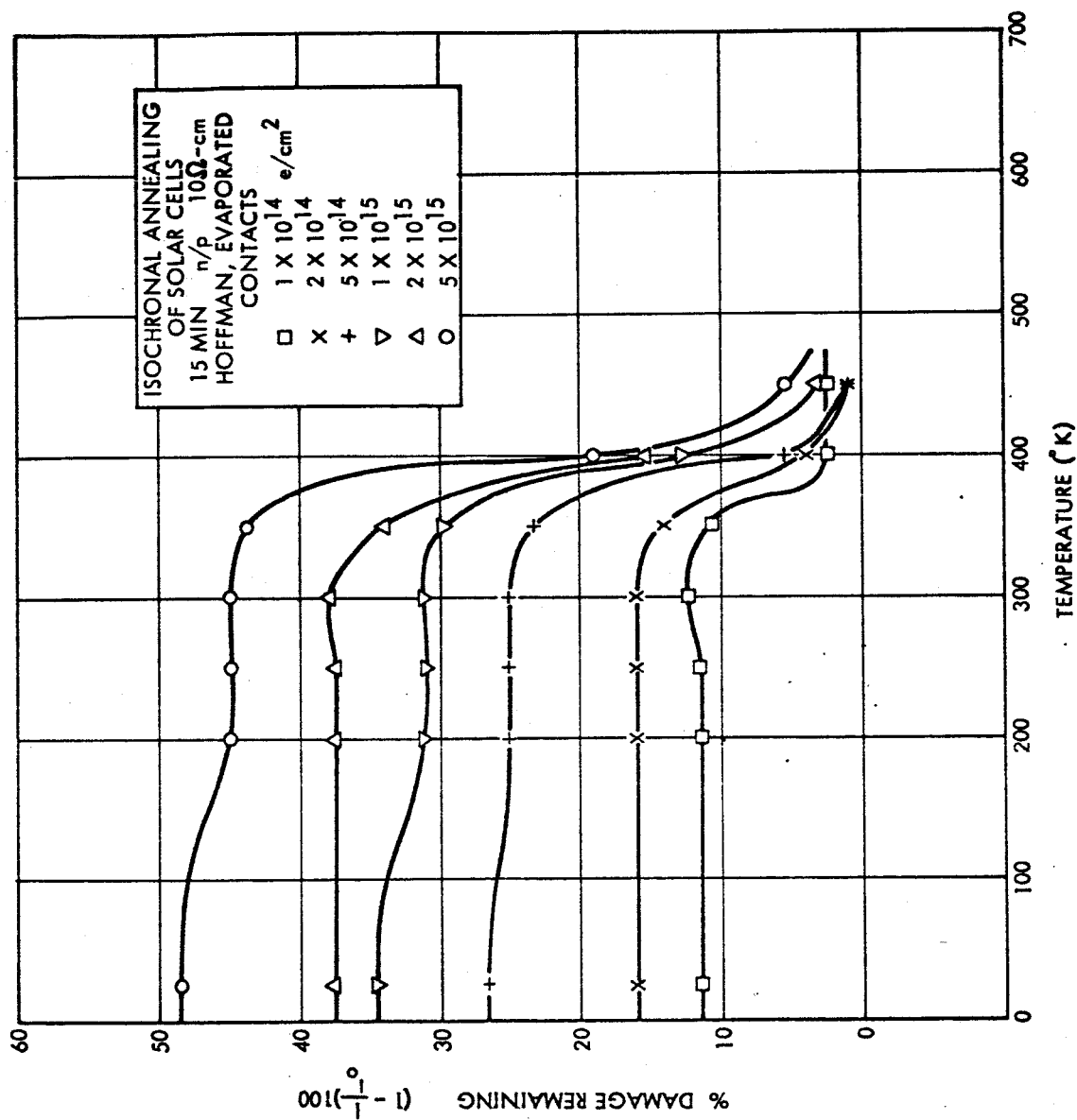


Figure 13. Isochronal Annealing of Hoffman n/p Solar Cells

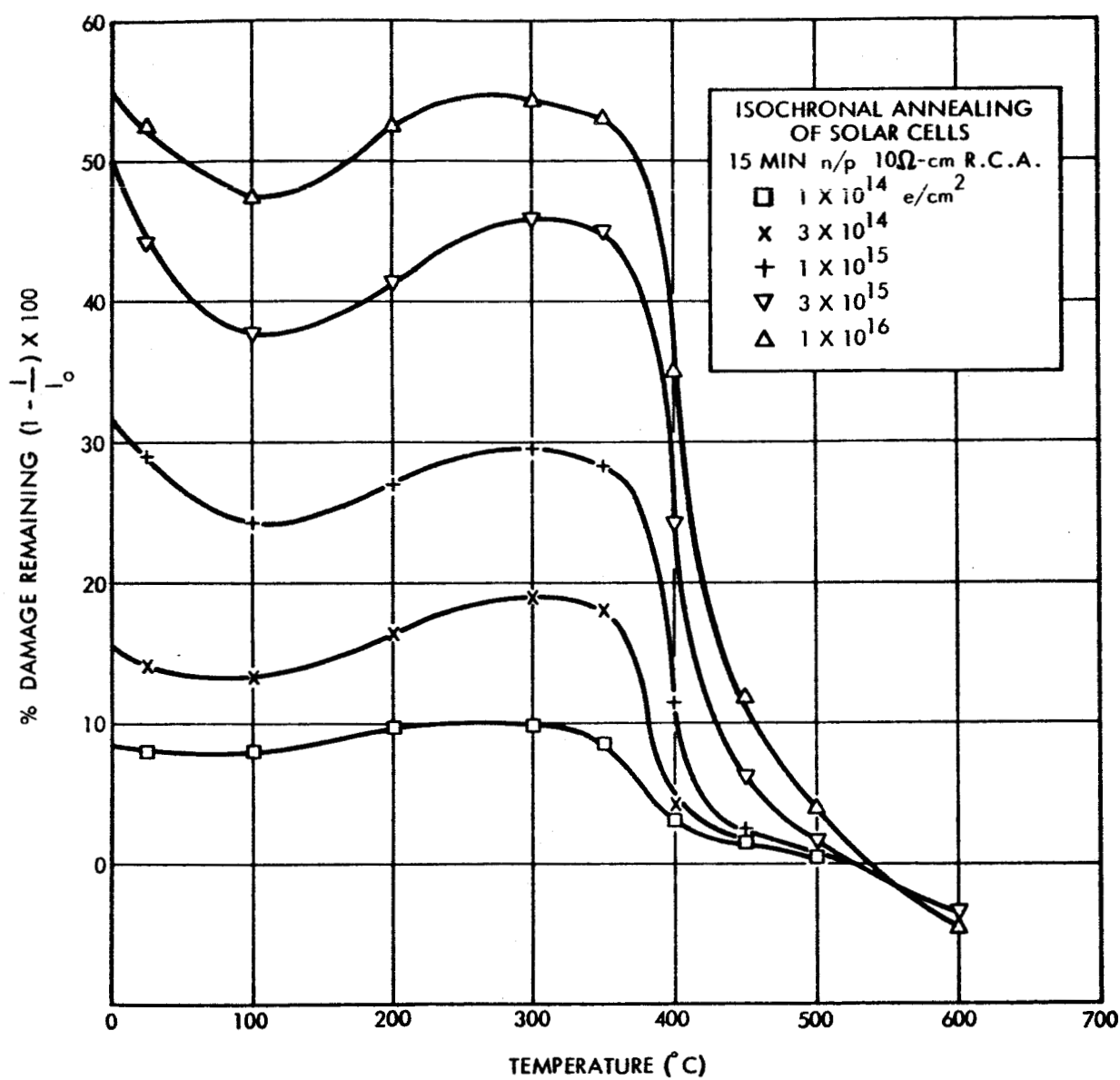


Figure 14. Isochronal Annealing of R.C.A. n/p Solar Cells

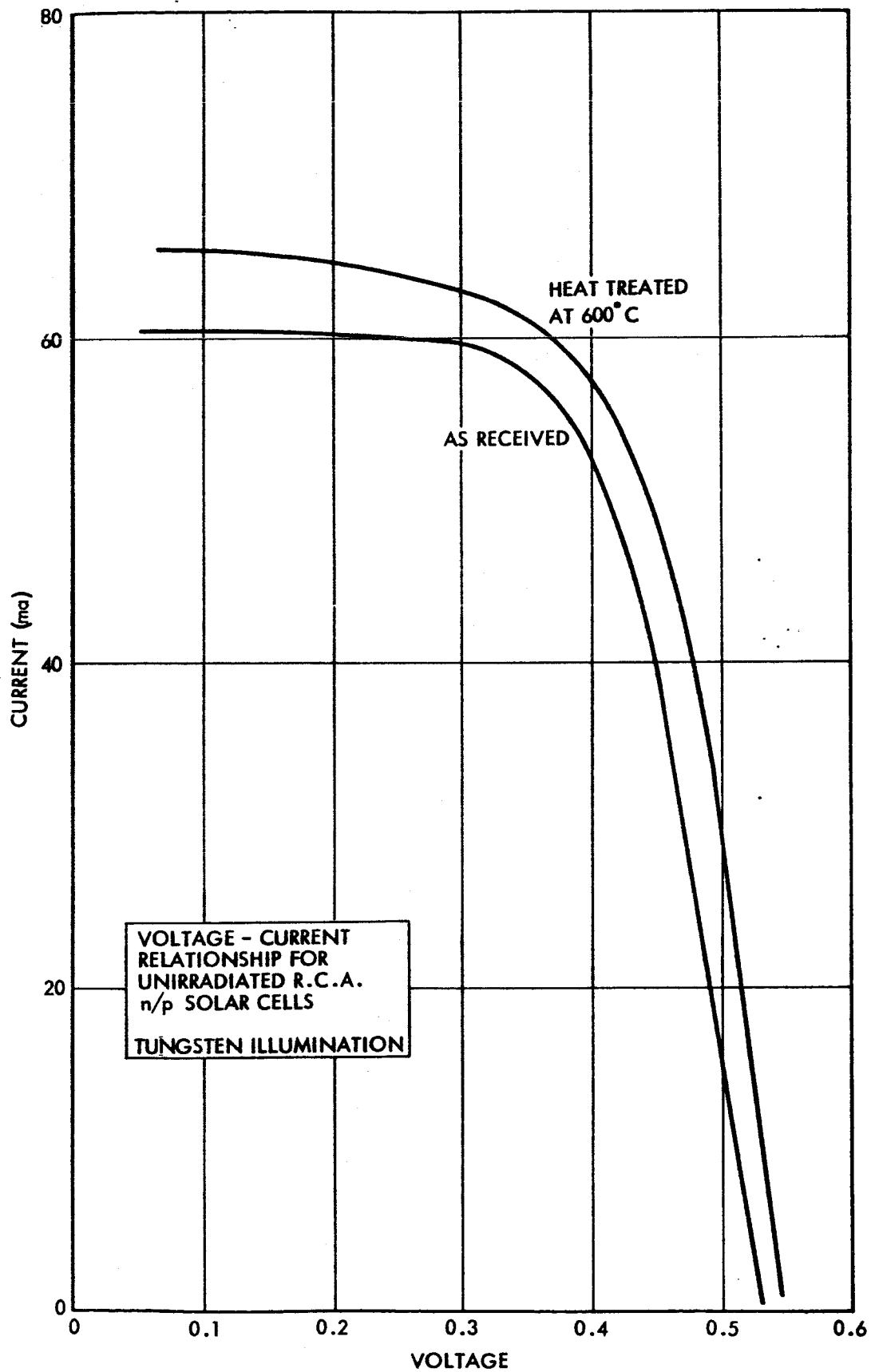


Figure 15. Heat Treatment of an Unirradiated R. C. A.
n/p Solar Cell

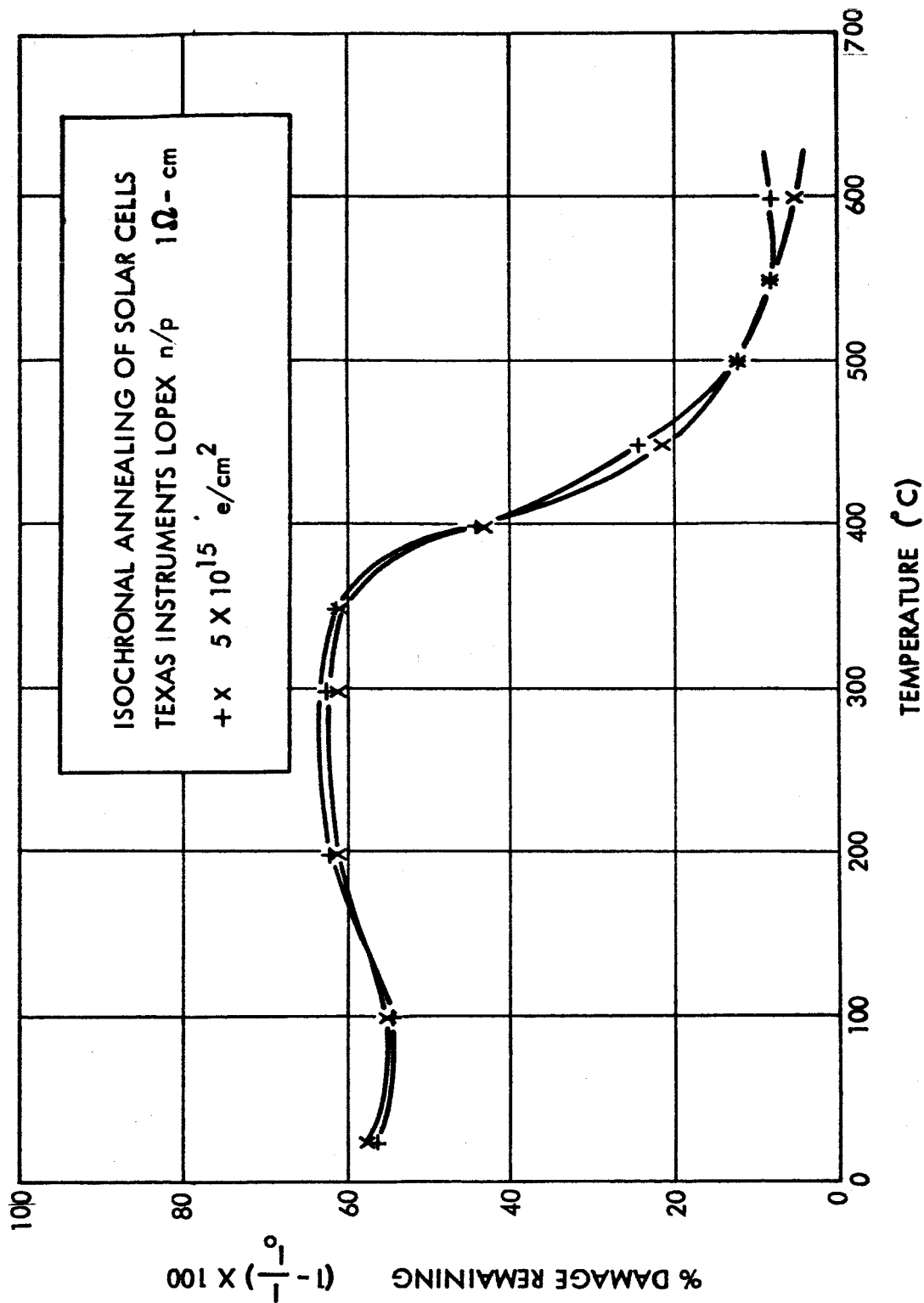


Figure 16. Isochronal Annealing of Texas Instruments n/p Solar Cells

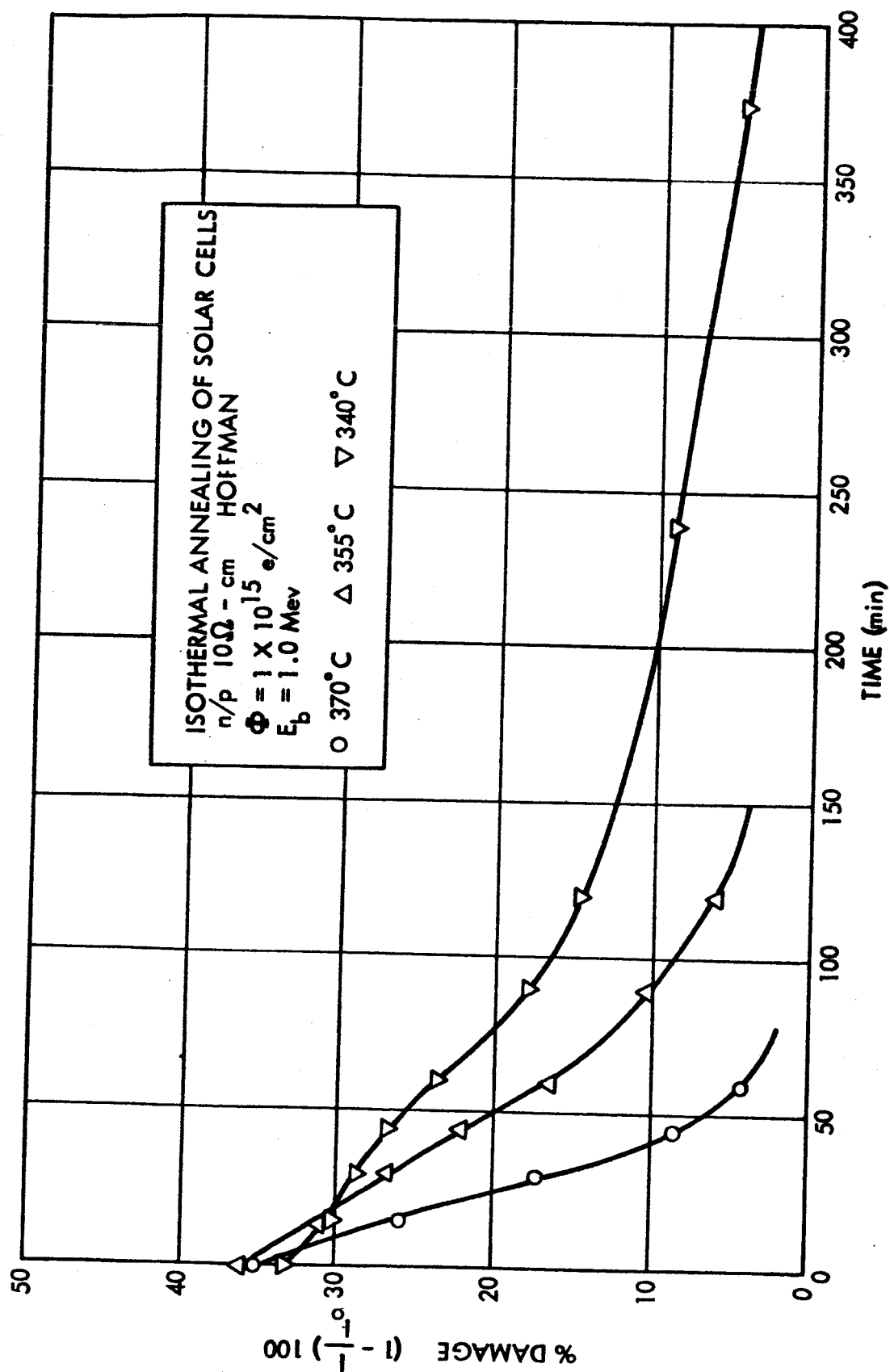


Figure 17. Isothermal Annealing of Hoffman n/p Solar Cells

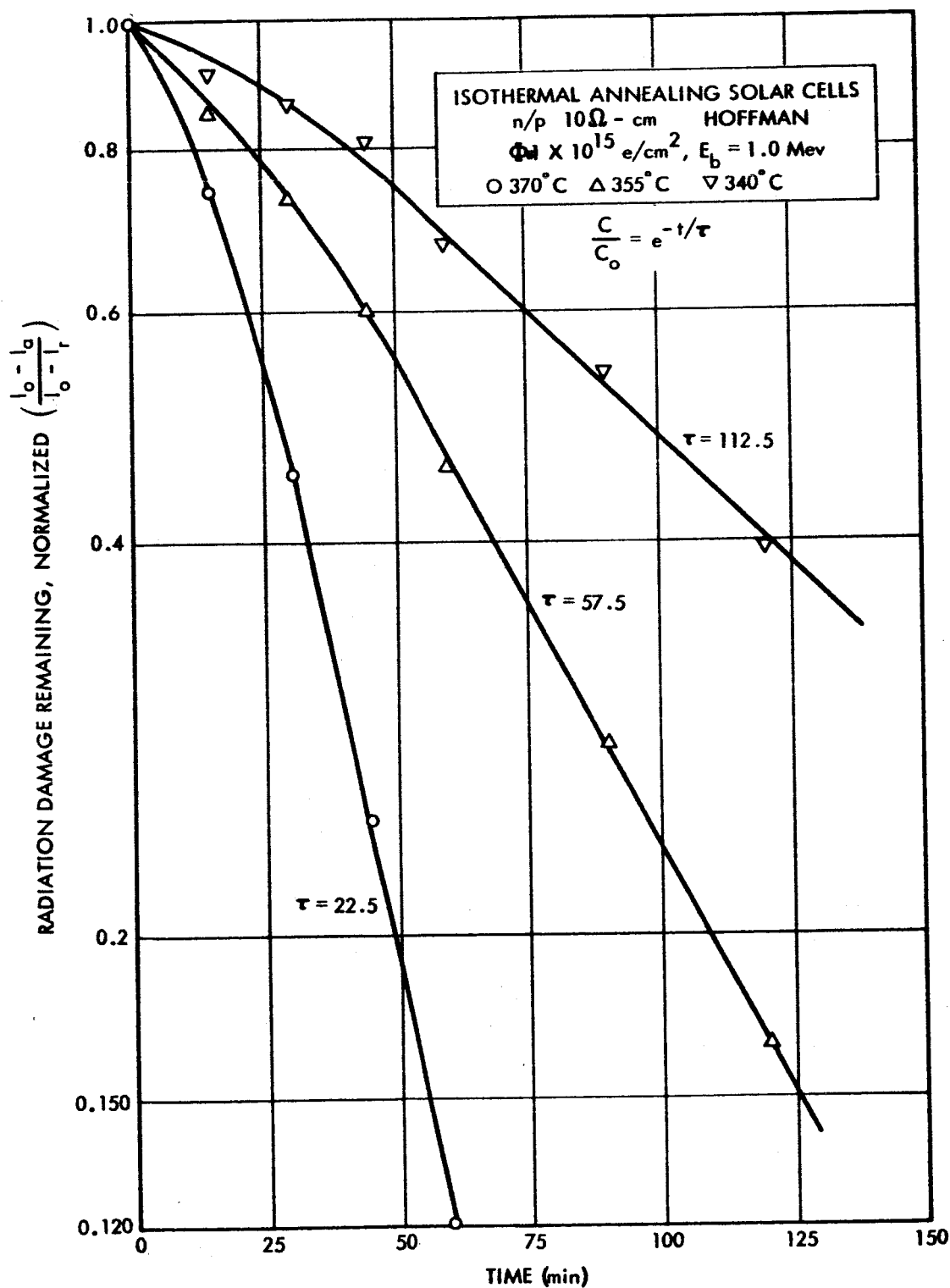


Figure 18. Isothermal Annealing of Hoffman n/p Solar Cells
(Semilogarithmic Plot)

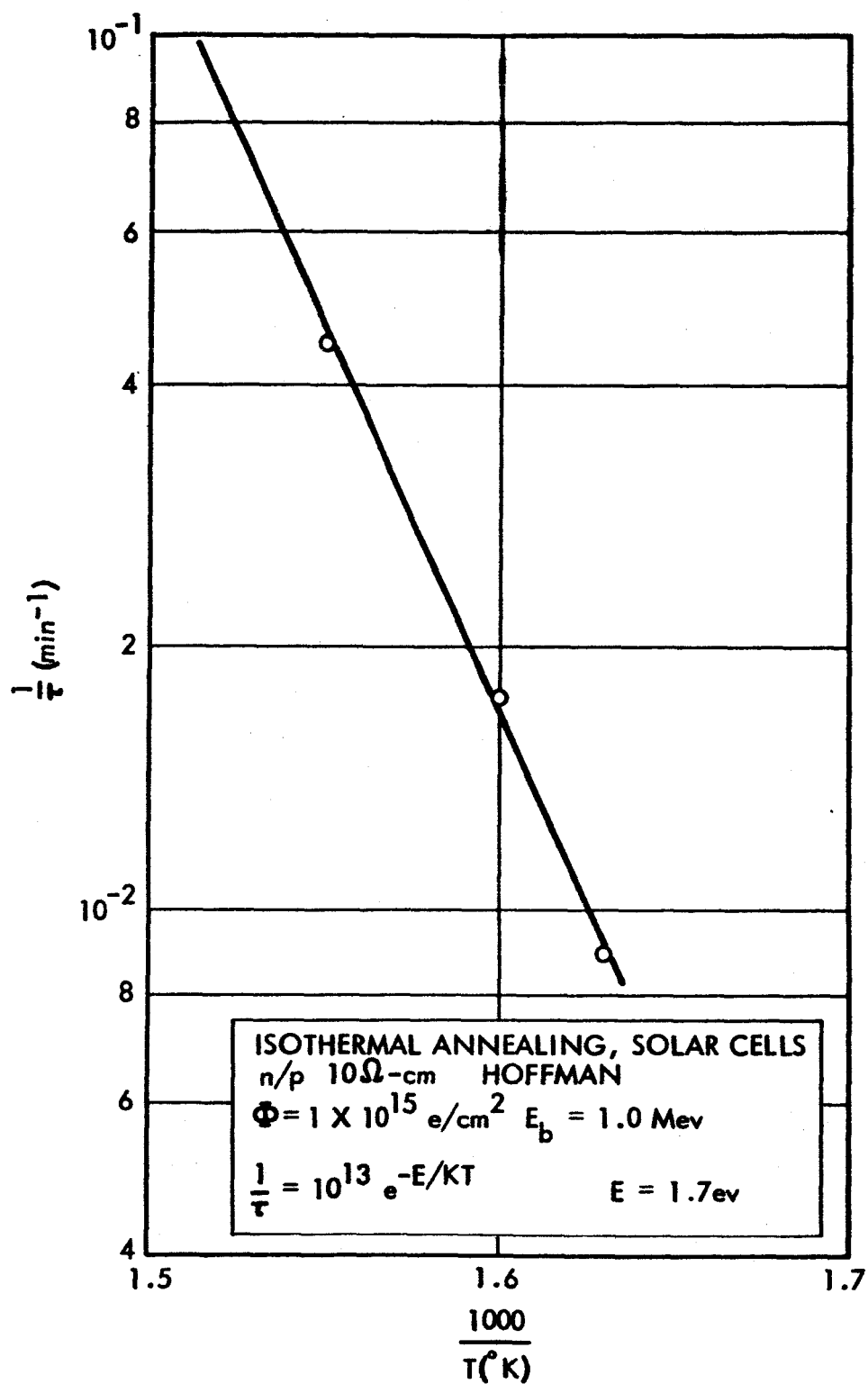


Figure 19. Arrhenius Plot for Hoffman n/p Solar Cells

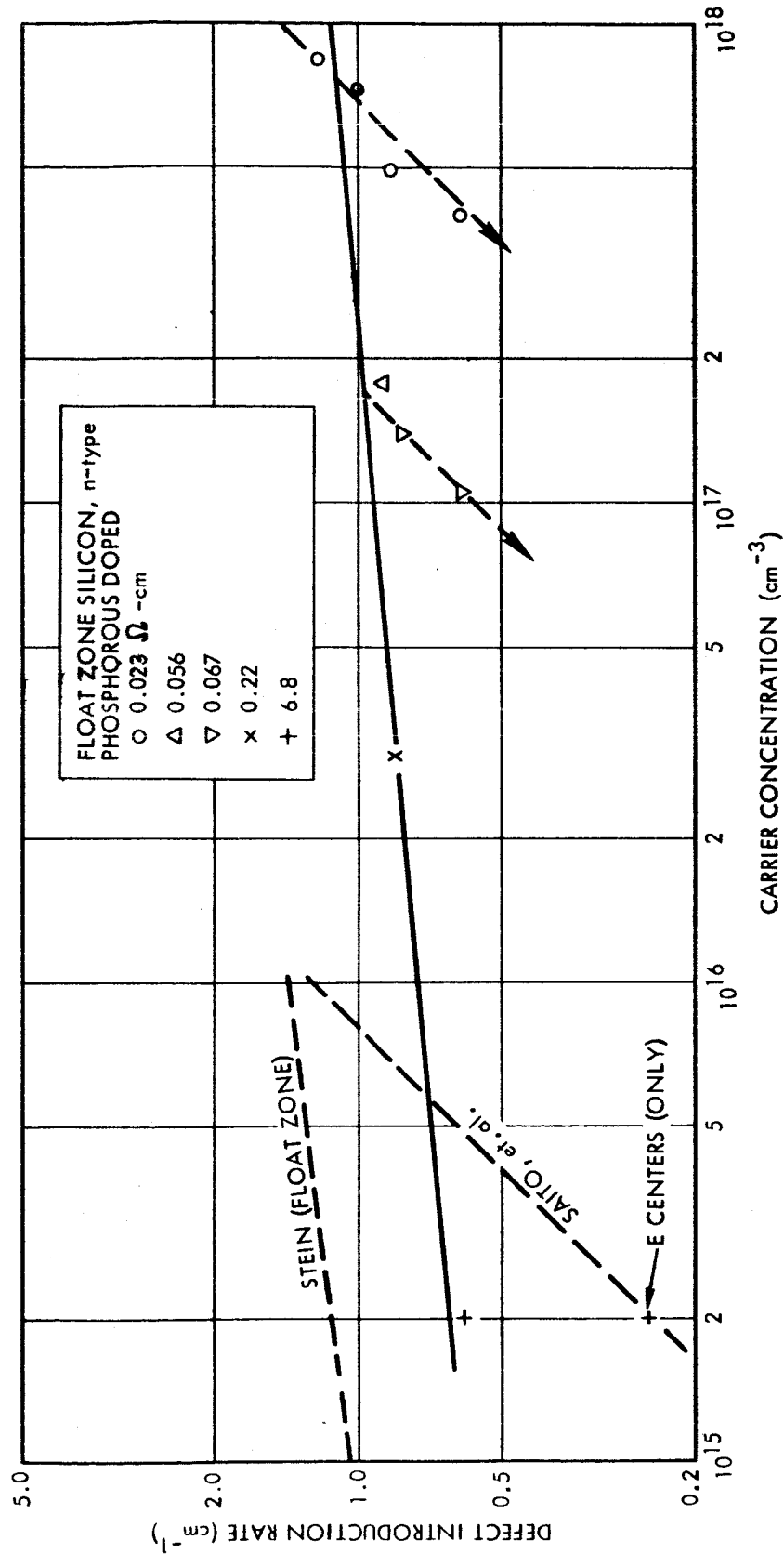


Figure 20. Electron Damage Defect Introduction Rate
for n-type Float Zone Silicon

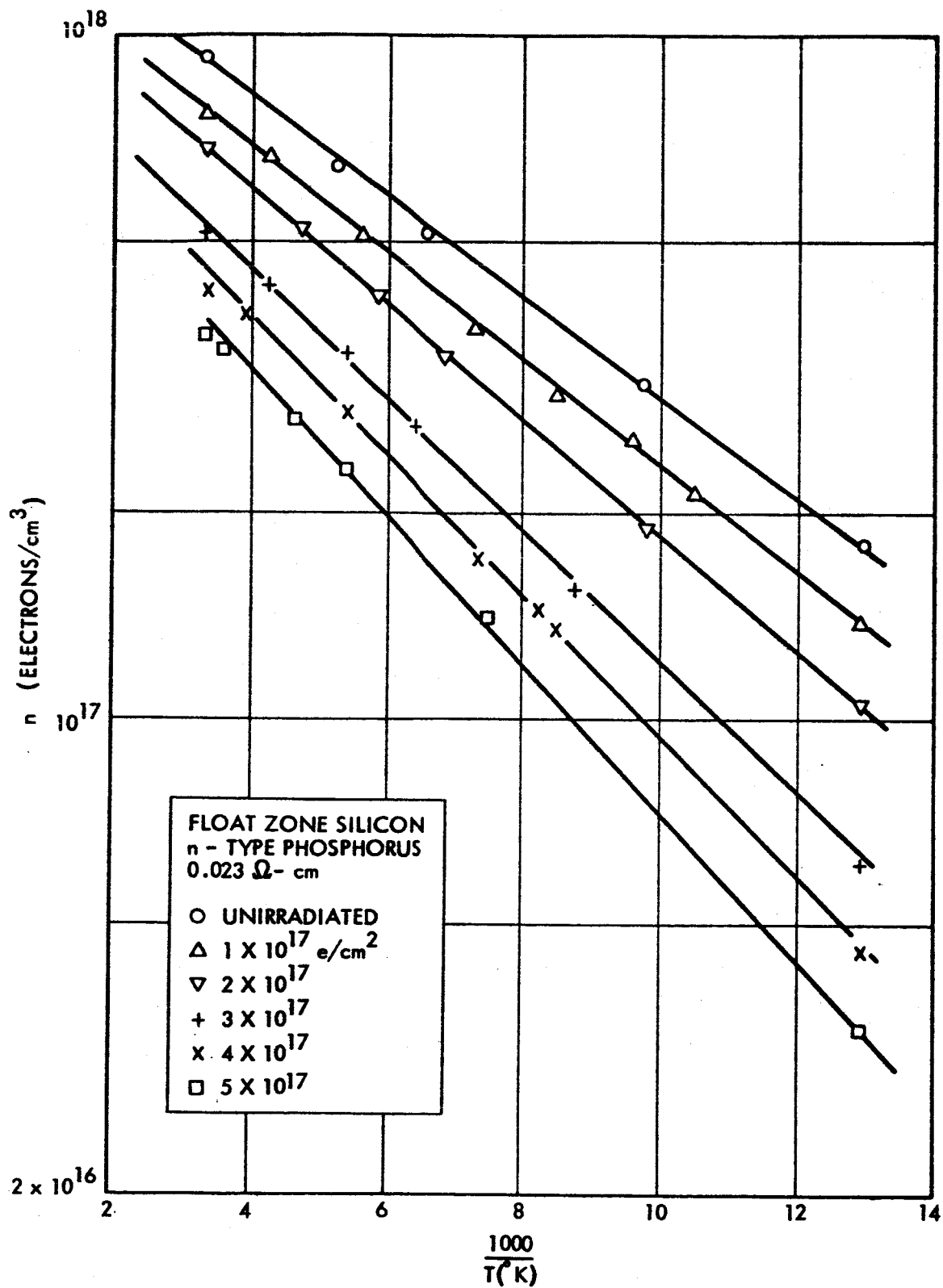


Figure 21. Carrier Concentration Versus Reciprocal Temperature for Electron Irradiated n-type Float Zone Silicon Sample

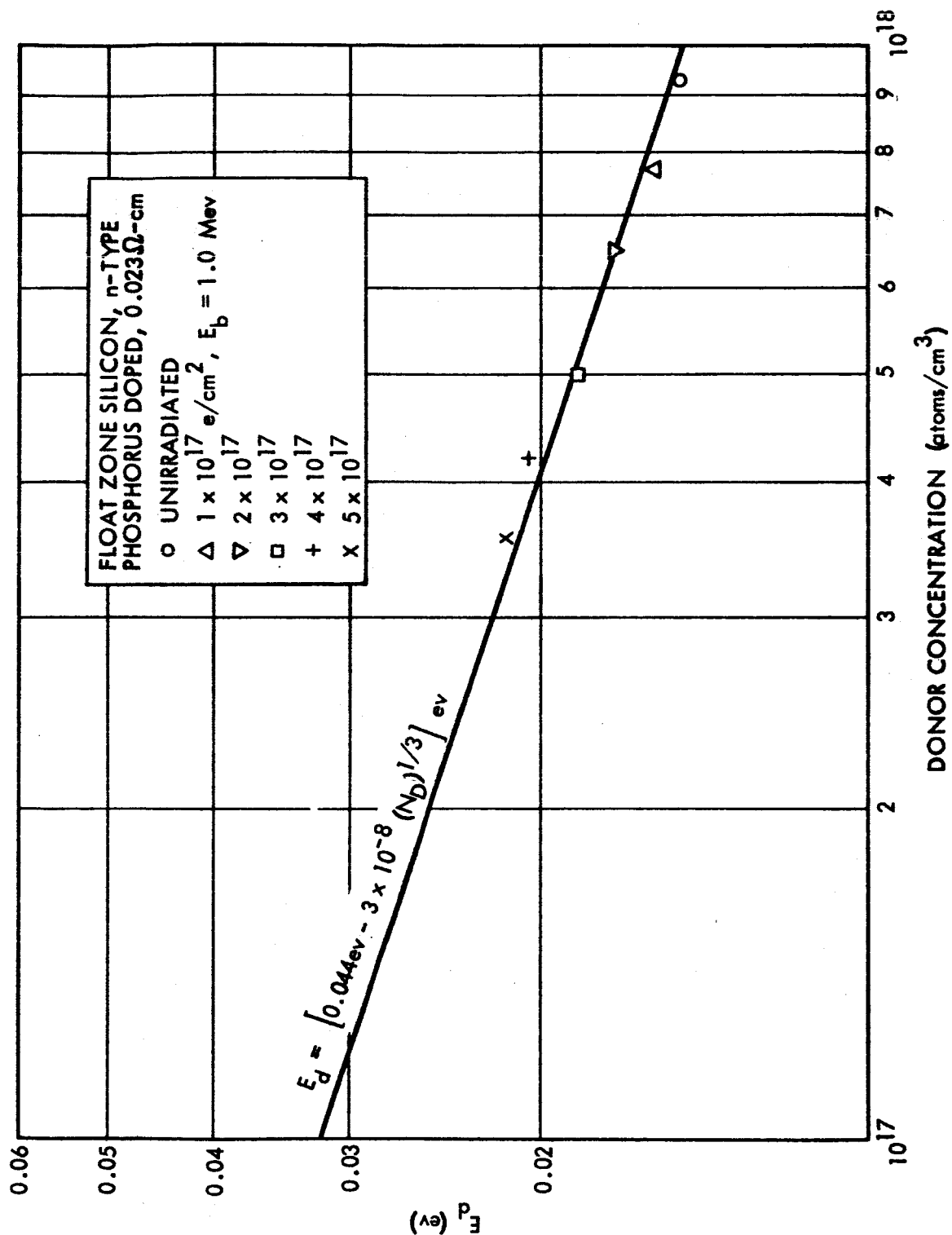


Figure 22. Donor Ionization Energy for an Electron Irradiated Float Zone n-type Silicon Sample

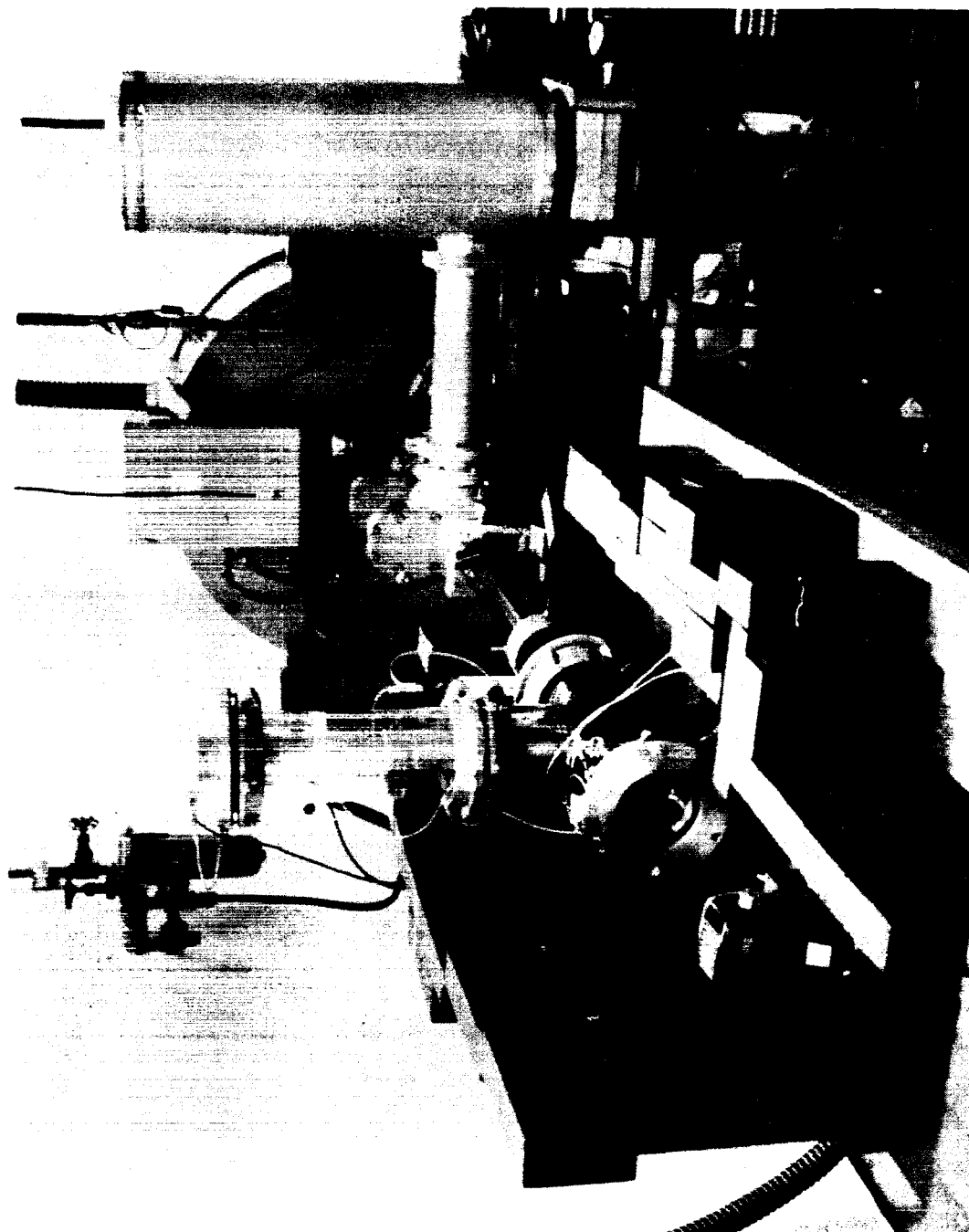


Figure 23. Experimental Apparatus for Electron Irradiation
of Solar Cell at Various Temperature



Figure 24. Close Up View of Solar Cell Irradiation Apparatus

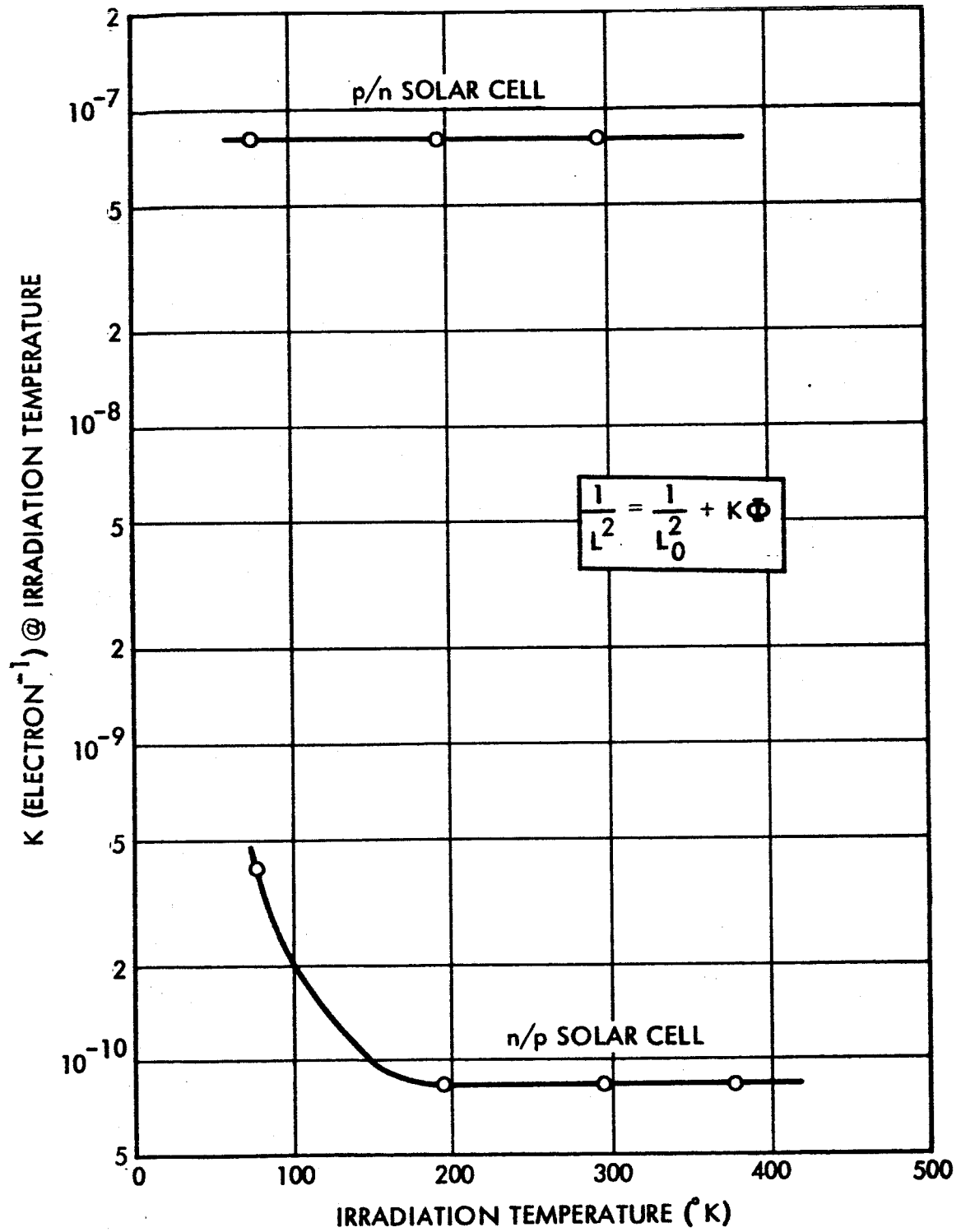


Figure 25. Damage Rate of Solar Cells for 1 MeV Electrons at Various Temperatures

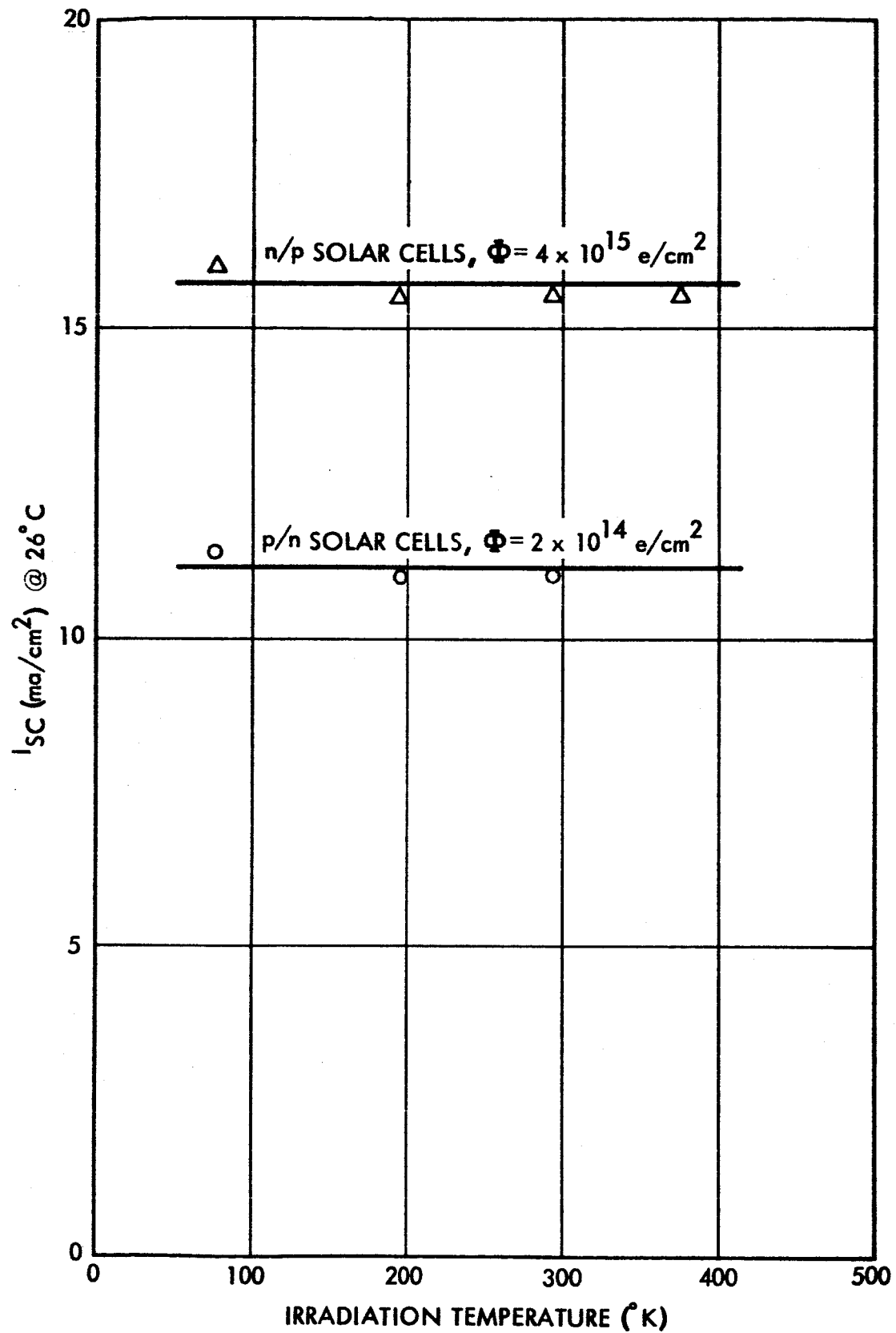


Figure 26. Room Temperature Short Circuit Currents for Solar Cell Irradiated at Various Temperatures

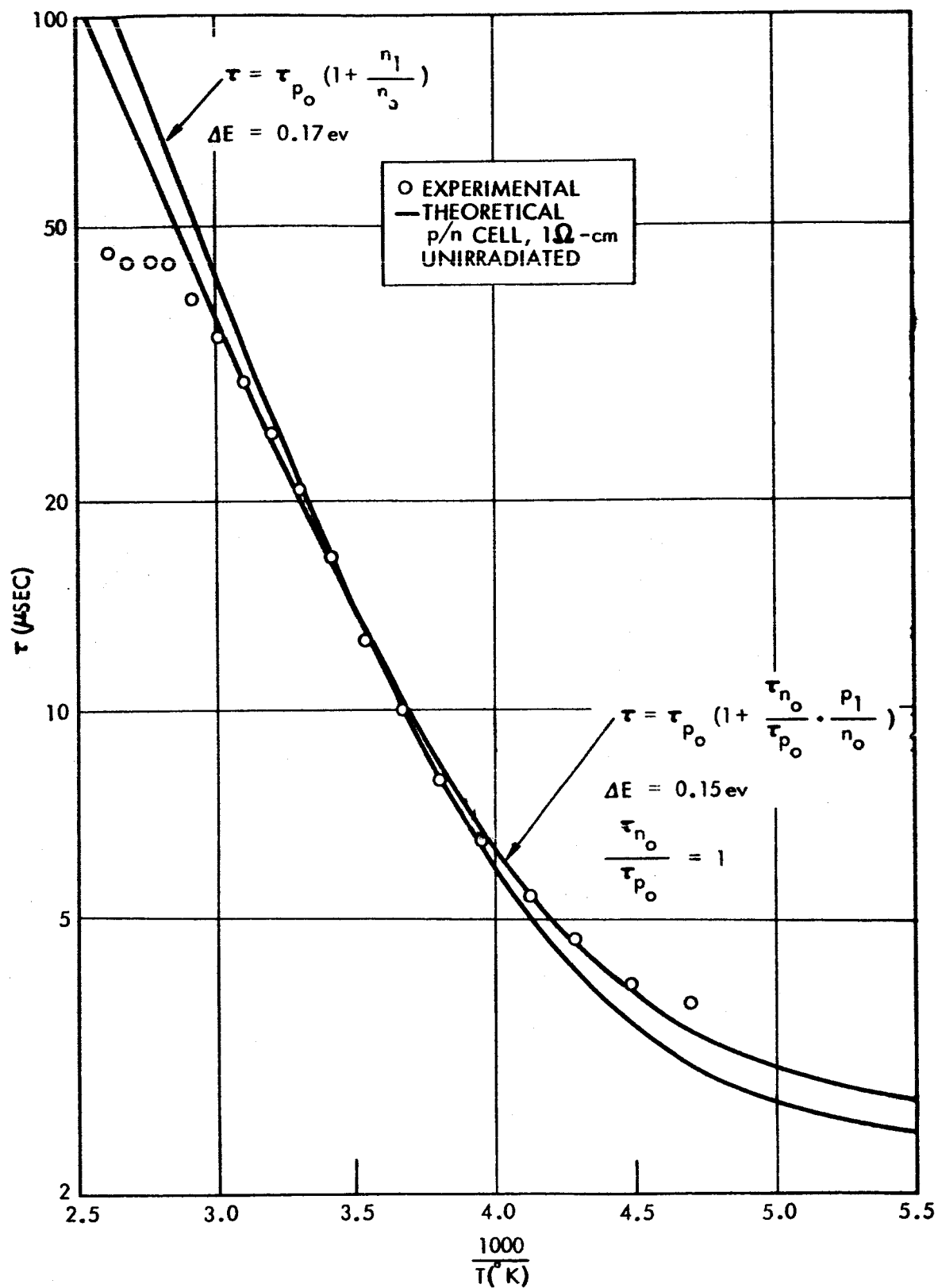


Figure 27. Dependence of Lifetime on Reciprocal Temperature, Unirradiated p/n Silicon Solar Cell

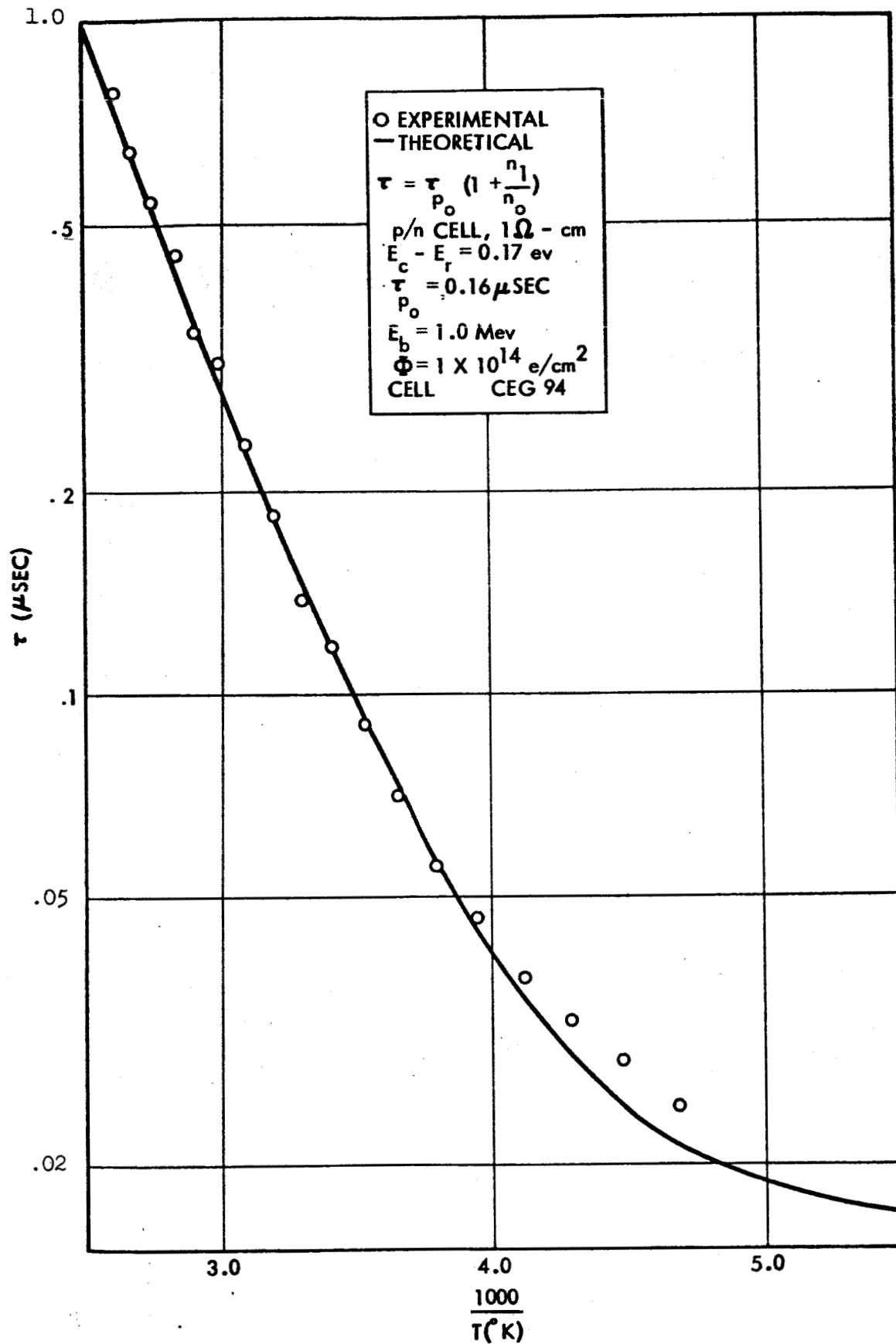


Figure 28. Dependence of Lifetime on Reciprocal Temperature, Electron Irradiated p/n Silicon Solar Cell

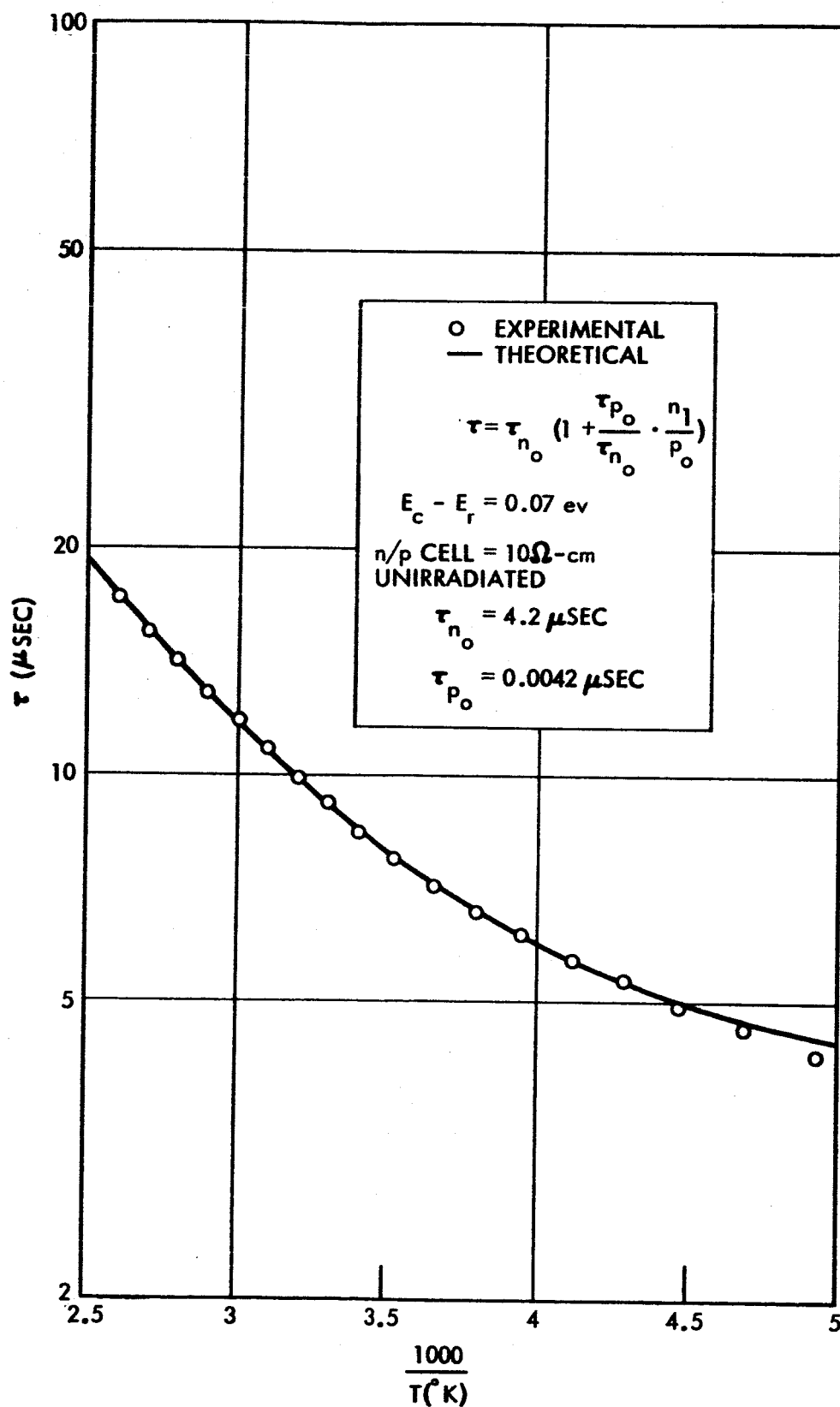


Figure 29. Dependence of Lifetime on Reciprocal Temperature
Unirradiated n/p Silicon Solar Cell

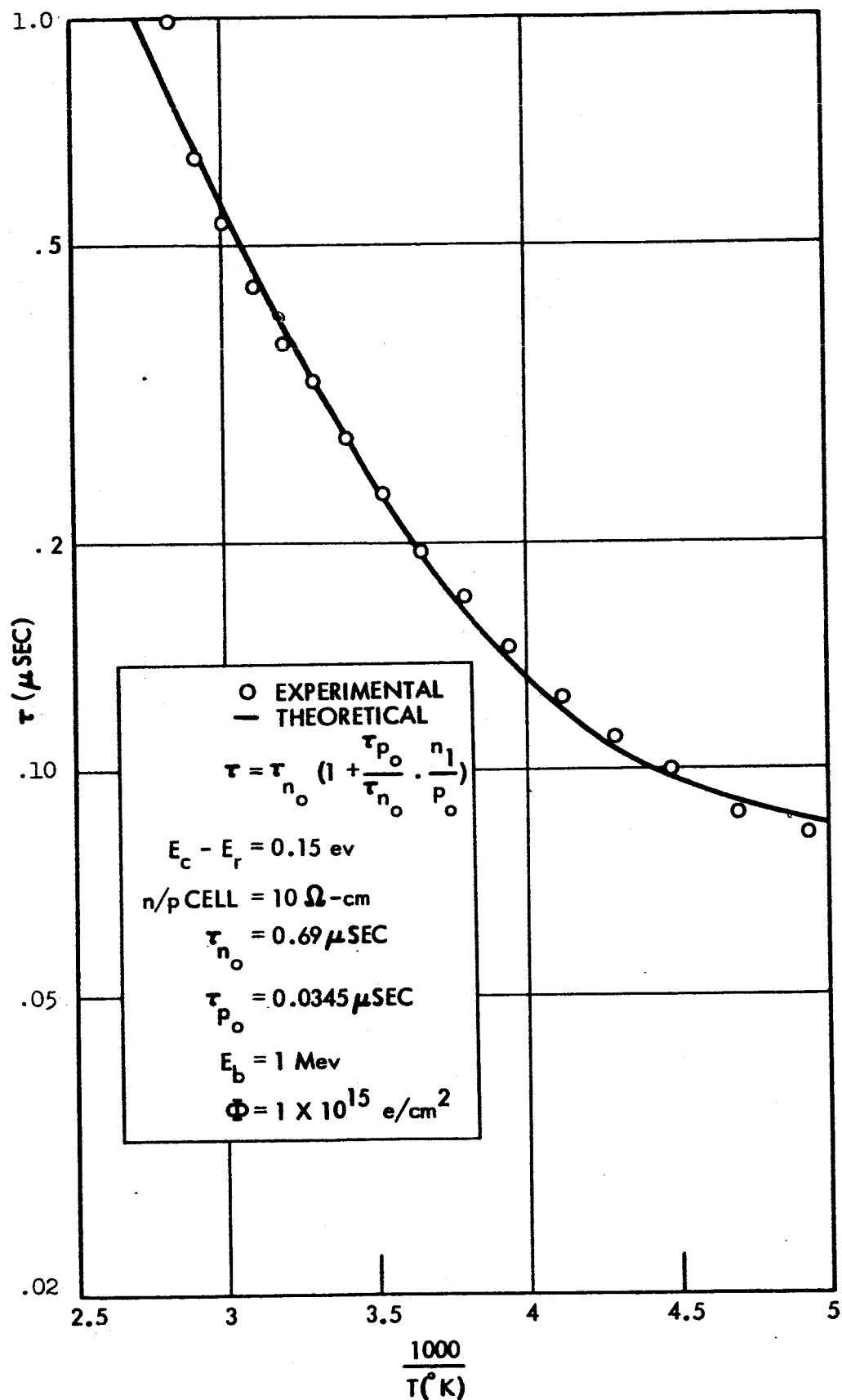


Figure 30. Dependence of Lifetime on Reciprocal Temperature
Electron Irradiated n/p Silicon Solar Cell

REFERENCES

1. G. K. Wertheim, Physical Review 105, 1730 (1957).
2. G. K. Wertheim, Physical Review 110, 1272 (1958).
3. G. N. Galkin, N. S. Rytova and V. S. Vavilov, Soviet Physics, Solid State 2, 1819 (1961).
4. J. A. Baicker, Physical Review 129, 1174 (1963).
5. R. G. Downing, J. R. Carter, Jr., and J. M. Denney. "Charged Particle Radiation Damage in Semiconductors, X: The Energy Dependence of Electron Damage in Silicon," Contract NAS5-3805, 4161-6004-KU-000 (3 September 1964).
6. G. D. Watkins and J. W. Corbett, Physical Review 121, 1015 (1961).
7. G. D. Watkins, Proceedings of the 7th International Conference on the Physics of Semiconductors, Dunod, Paris (1964).
8. D. E. Hill, Physical Review 114, 1414 (1959).
9. J. R. Carter, Jr., Journal of Chemistry and Physics of Solids, to be published.
10. B. Goldstein, N. Almeleh, and J. J. Wysocki, R.C.A. Semiannual Report, July 1965, Contract NAS5-9131.
11. V. M. Molovetstskaya, G. N. Galkin, and V. S. Vavilov, Soviet Physics, Solid State 4, 10018, 1962.
12. E. Sonder and L. C. Templeton, Journal of Applied Physics 36, 1811 (1965).
13. Personal Communication from N. Almeleh
14. G. Binski and W. M. Augustyniak, Physical Review 108, 645 (1957).
15. J. W. Corbett, et al., Physical Review 121, 1015 (1961).
16. H. Saito and M. Hirata, Japanese Journal of Applied Physics 2, 678 (1963).
17. E. Sonder and L. C. Templeton, Journal of Applied Physics 34, 3295 (1963).
18. P. H. Fang, "Thermal Annealing of Radiation Damage in Solar Cells," NASA Report X-713-65-468, November 1965.

19. E. Baldinger and M. Lenzlinger, Solid State Electronics 9, 287 (1966).
20. Personal Communication from B. Goldstein.
21. A. J. Stein, "Introduction Rate of Electrically Active Defects in n-type Silicon by Nuclear Radiation, Sandia Report SC-R-65-938 (1965).
22. G. L. Pearson and J. Bardeen, Physical Review 75, 865 (1949).
23. P. P. Debye and E. M. Conwell, Physical Review 93, 693 (1954).
24. R. Gremmelmaier, Proceedings of the IRE 46, 1045 (1958).
25. G. K. Wertheim, Physical Review 115, 568 (1959).
26. R. L. Novak, "Temperature and Energy Dependence of the Introduction and Annealing Rates of Electron-Induced Defects in n- and p-type Silicon," Ph.D. Thesis, Univ. of Pennsylvania (1964).
27. R. N. Hall, Physical Review 83, 387 (1952).
28. W. Shockley and W. T. Read, Jr., Physical Review 87, 835 (1952).
29. G. W. Ludwig and R. L. Watters, Physical Review 101, 1699 (1956).